A Proposed Formation of Unique Crystallographic Ikaite as a Key Proxy for Identifying Frigid Ancient Climates in Creede, Colorado During the Late Oligocene

Amir Romly

Senior Honor Thesis
Department of Geological Sciences
University of Colorado Boulder

Defended on 4/10/2024

Thesis Advisor: Dr. Lizzy Trower

Thesis Committee Members:

Dr. Lizzy Trower (Department of Geological Sciences)
Dr. Brian Hynek (Department of Geological Sciences)
Dr. Katherine Lininger (Department of Geography)

I. Abstract

The metastable pseudomorph of calcium carbonate known as ikaite ($CaCO_3.6H_2O$) is a reliable tool for recognizing frigid ancient climates. Its recognition is aided by the unique guttulatic structure. This structure appears as ellipsoidal overgrowths surrounding pseudohexagonal to ellipsoidal cores. These cores are surrounded by more Mg-rich sparry or micritic cement.

This study employs Transmitted Light (TL) microscopy, Cathodoluminescence (CL) microscopy paired with Plane Polarized Light (PPL) and Cross Polarized Light (XPL) microscopy, alongside stable isotope $\delta^{13}C$ and $\delta^{18}O$ analyses. These are used to investigate the crystallography of ikaite. The aim is to discern the frigid ancient climate of Creede, Colorado during the Oligocene period. A key focus is on identifying the guttulatic crystal structure of ikaite. Traditionally, it has been described as possessing a sole pseudo-hexagonal core with overgrowth in various cold locations. However, our examination reveals core variations in Creede. These include tear-drop, oval, triangular, circular almond, and irregular rounded corner shapes. This indicates the presence of guttulatic structures as the second most abundant form. Furthermore, our analysis of the water chemistry of ancient Lake Creede suggests complexities in interpretation. We observe a non-luminescent core, the shape of which is consistent with vaterite. We hypothesize its formation in a highly oxygenated environment. Subsequent overgrowth with lighter orange CL luminescence suggest a transition to a low-oxygen environment. Macroscopic observations of ikaite pseudomorphs, specifically glendonite formation, offer insights of environmental conditions. The transformation of guttulatic crystals into stable vaterite hexagonal cores with overgrowth, accompanied by sparry calcite filling, suggests warming and loss of water. Calcite with cleavage angles exceeding 78° and 102° indicates temperatures surpassing 8°C of the stability range of ikaite. While a dislocation of guttulatic crystal is hypothesized to be deformed during uplift event

such as the Neogene uplift and Rio Grande incision. Analysis of $\delta^{13}C$ and $\delta^{18}O$ values are consistent with a cold-water environment during the Oligocene. Low $\delta^{13}C$ values imply organic carbon incorporation, possibly influenced by decaying organic matter in mud deposits. Higher $\delta^{18}O$ values suggest colder climate conditions, indicative of a cold and dry evaporative ancient Creede Lake approximately 26.9 million years ago. This comprehensive approach enhances our understanding of Creede's paleoclimate and geological evolution.

Table of Contents:

II. Introduction and Literature Survey

1.1. Importance of Calcium Carbonate

Understanding Earth's past climate is a crucial endeavor, not only for historical curiosity but also for improving our predictions of future climate dynamics. Paleoclimate studies offer a unique window into how environmental conditions changed over a variety of timescales, including the exceptionally long ones. Paleoclimate studies draw upon a rich array of instrumental proxies, ranging from fossils like diatoms, foraminifera, corals, tree rings, and pollen to non-biogenic materials such as calcium carbonate. While fossils provide valuable insights into past climates, the exploration of climate dynamics through calcium carbonate represents a particularly intriguing avenue of research.

Calcium carbonate, denoted as $CaCO_3$, represents a mineral ubiquitously found and precipitated in various environments. For example, stalagmites and stalactites, distinctive cave formations, form in locations where water dissolves overlying limestone, subsequently redepositing calcium carbonate along cave ceilings or floors (NOAA). Furthermore, the regression and transgression of sea levels can also create strata of calcium originating from the precipitation of carbonated shells or benthic organisms in marine environments.

Most of the precipitation of calcium carbonate is most favorable within a temperature range characteristic of warmer conditions in shallow environment. In Earth's oceans, the Carbonate Compensation Depth (CCD) marks the point where the rates of calcium carbonate supply and dissolution are in balance. Below the CCD, typically below 15,000 feet (4500 meters), calcium carbonate particles do not accumulate due to the lack of preservation. However, despite the association of $CaCO_3$ precipitation with warm waters, one form of calcium carbonate

known as ikaite has been observed to precipitate at the interface of shallow water columns in cold environments in both the marine and terrestrial realms.

1.2. Ikaite as an Alternative Proxy to Frigid Temperature.

Despite the stability of carbonate in warmer temperatures, a unique form of calcium, known as ikaite, remains stable in colder environments. Ikaite ($CaCO_3 \cdot 6H_2O$), identified as a metastable pseudomorph of calcium carbonate, serves as a dependable proxy for identifying ancient climates characterized by cold conditions. Ikaite exhibits metastability under natural conditions, primarily in low temperatures approaching the freezing point of water. Typically, it develops into centimeter-sized single euhedral crystals or stellate crystal aggregates when close to the sediment-water interface as proposed by Scheller et al. (2022) (Figure 1). However, upon temperature rise or changes in pore-water chemistry, ikaite rapidly transforms into calcite (Pauly, 1963; Swainson and Hammond, 2001).

This replacive calcite is commonly characterized by guttulatic microfabric. This includes the presence of pseudo-hexagonal core crystals with ellipsoidal overgrowths; these crystals are subsequently engulfed by secondary high-Mg sparry or micritic cement (Scheller et al., 2022). The unique characteristics of ikaite as an early form of calcium carbonate offer a sophisticated way to identify certain cold settings, leading to more accurate results and a fresh viewpoint on climate studies. Furthermore, certain conditions involving high alkalinity, phosphate concentration levels are necessary for the formation of these minerals. (Suess et al., 1982; Bischoff et al., 1993; Buchardt et al., 2001; Swainson & Hammond, 2001; Zhou et al., 2015)

There are numerous papers that support this model of ikaite formation and destabilization. For example, low temperatures (<8°C) and high phosphate and alkalinity concentrations (to prevent calcite and aragonite formation) are necessary chemical conditions for

ikaite to reach metastability (Suess et al., 1982; Bischoff et al., 1993; Buchardt et al., 2001; Swainson & Hammond, 2001; Zhou et al., 2015). According to Bischoff et al. (1993), ikaite also becomes more soluble at higher temperatures, making it harder to precipitate. Studies conducted by Huggett et al. (2005) and Field et al. (2017) have shown that ikaite crystals only naturally form at temperatures below 9°C. Additionally, Hu et al. (2014) observed that salinity and pH may significantly influence ikaite precipitation, as evidenced in their investigations using artificial seawater. The idea that ikaite only naturally exists in water temperatures between 1.9°C and 7.8°C was also supported by a number of previous studies (Pauly, 1963; Suess et al., 1982; Buchardt et al., 1997)

Marine sedimentary ikaite is frequently found in modern shelf environments, usually between 3 and 20 meters below the sediment-water interface, especially in the vicinity of the sulphate-methane transition zone (Schubert et al., 1997; Lu et al., 2012). These occurrences coincide with porewater temperatures below 8°C (Zhou et al., 2015), consistent with other observations of the necessary environmental conditions for ikaite formation. There are multiple macrohabits of ikaite crystals that can be found within these environments such as stellate aggregates, bi-pyramidal/prismatic crystals, thinolite/radial bladed tufa, porous massive tufa, porous massive crusts, and speleothem crust/coating (Figure 2).

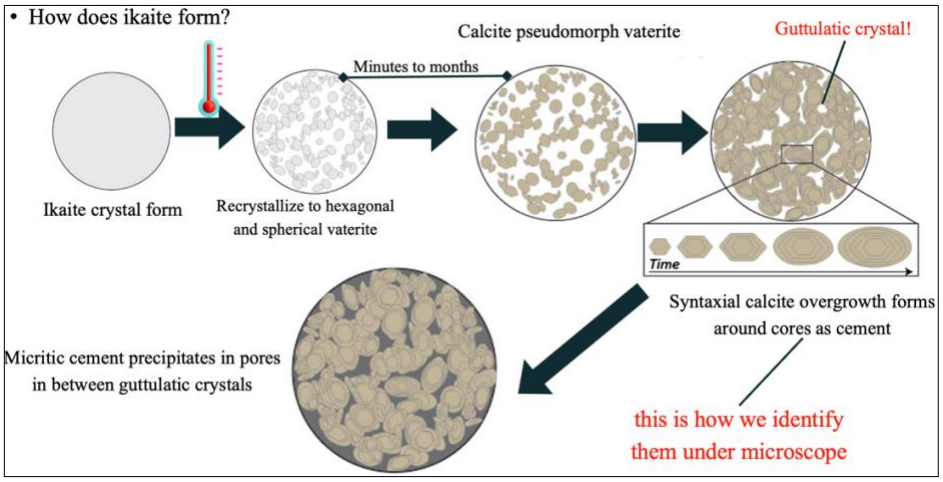

Figure 1. Proposed drawing of ikaite crystal forming ellipsoidal overgrowth around the core known as guttulatic crystal. (Modified after Scheller et al., 2022).

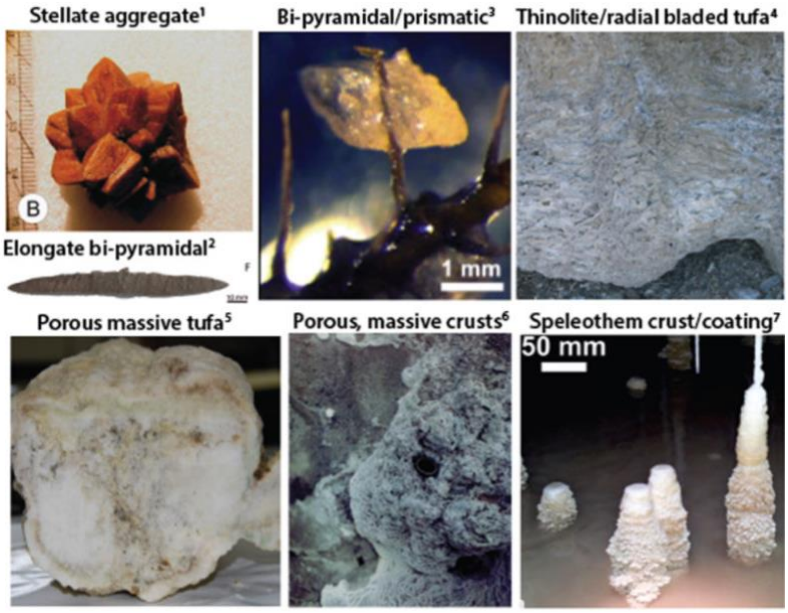

Figure 2. Examples of different macrohabits of ikaite crystals. (Modified after Selleck, B.W., Carr, P.F., and Jones, B.G., 2007)

1.3. Presence of Glendonite as a Part of Ikaite Formation:

Glendonite, which is sometimes confused for a mineral, is actually a pseudomorph of gypsum that follows ikaite (Larsen et al., 1994b) as seen in Figure 3. Although ikaite and glendonite have been known for a while, the relationship between ikaite and glendonite was only conclusively proven after glendonite-like crystal aggregates were found in organic-rich sediments of the Bransfield Strait off the Antarctic Peninsula (Suess et al., 1982). Ikaite is a significant indication of glaciomarine and cold deep-water settings due to the restricted temperature limits that are conducive to its development (Selleck et al., 2007). Glendonite has therefore been used to support frigid-water depositional environments in ancient records of geology and has important paleoclimatic implications (James et al., 2005; Wang et al., 2017).

It has been suggested that ikaite pseudomorphs that are mostly made of low-Mg calcite, or "glendonite," can be used as a substitute for cold depositional water conditions from the past

(De Lurio and Frakes, 1999; Swainson and Hammond, 2001; Selleck et al., 2007). For example, the near-freezing marine temperatures that occur throughout, in between, and after global glaciations have been confirmed by Neoproterozoic glendonite (James et al., 2005; Dempster and Jess, 2015; Wang et al., 2020). Although glendonite texture is not well defined, it is generally understood to represent an ikaite pseudomorph that is occasionally characterized by stellate crystals on the size of centimeters (e.g., Selleck et al., 2007). According to Jafarzadeh and Burnham (1992), some of these formations may in fact be pseudomorphs of evaporite minerals, which likewise have stellate or bipyramidal crystal structures.

The $\delta^{13}C$ values of many ikaite and glendonite specimens fall within the range of -10‰ to -25‰, much lower than expected for carbonate minerals forming in isotopic equilibrium with seawater, suggesting that biogeochemical processes might be related to mineral formation. Given the ambiguity often associated with stable carbon isotope signatures, additional proxies are necessary to ascertain whether mineral formation resulted from sulfate reduction or anaerobic oxidation of methane. Regrettably, such reconstructions are further complicated by uncertainties regarding the factors influencing the transformation of ikaite into glendonite. This is because the transformation involved diagenesis, presence of organic matter, water chemistry and many more. (Rye et al., 2000)

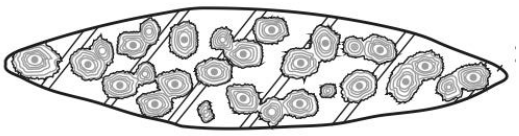

Figure 3. Proposed a close-up diagram of a rice-grain shape of glendonite, a pseudomorph after ikaite, encapsuling the guttulatic crystal and sparry calcite (Modified after Vickers et al., 2018).

2.1.Area of Study: Creede, Colorado

This study will delve into the mechanisms underlying ikaite precipitation in Creede, Colorado. The Creede caldera, formed approximately 26.9 million years ago, was once a moderately saline closed-basin lake nestled in the central San Juan Mountains of Colorado. It stands as an exceptionally preserved example of a large resurgent caldera, renowned for its association with world-class epithermal Ag-Pb-Zn deposits (Steven and Ratté, 1965; Bethke and Hay, 2000). Among the nine subsidence structures in the central San Juan caldera cluster, Creede caldera, ranging in age between 28.6 and 26.9 million years, is the youngest (Steven and Ratté, 1965; Emmons and Larsen, 1923).

Creede caldera serves as the culmination of late Oligocene volcanic activity in the San Juan magmatic region of the Southern Rocky Mountain volcanic field (SRMVF) in Colorado and New Mexico. The late Neogene uplift that followed, together with the Rio Grande's incision, allowed the soft intracaldera sediments in Creede caldera to be exposed while maintaining its distinctive form (Rye et al., 2000). This area has a wealth of minerals and rocks, including quartzite, pyrite, zinc, plumbum, argentum, carbonate rocks, and tuff. It is distinguished by several geological indications of volcanic formation, subsidence, and persistent precipitation (Rye et al., 2000). As a result, Creede became a major location for coring and drilling operations, notably those carried out by the Continental Scientific Drilling Project in the United States. Apart from its economic importance, Creede has great geological attraction, which makes it a perfect setting for researching past climates (Rye et al., 2000).

2.2. Chronology of Lake Creede Formation

Lake Creede, situated within the confines of the Creede caldera, owes its origin to the resurgent silicic caldera, a product of the Snowshoe Mountain Tuff eruption. The resurgent dome and annular moat of the caldera have been exceptionally preserved (Lipman, 2008). The San Juan Mountains, remnants of a mid-Tertiary composite volcanic plateau, were once blanketed by a silicic batholith, giving rise to a pronounced regional gravity low (Plouff and Pakiser, 1972). The earliest eruptions, occurring around 35-30 million years ago, formed intermediate composition stratovolcanoes, gradually overlain by ash-flow sheets emanating from clustered caldera sources approximately 30-26 million years ago (Lipman, 2008). The subsequent bimodal suite, dominated by basalts from approximately 26-5 million years ago, coincided with regional extension associated with the opening of the Rio Grande rift.

Creede caldera, among the nine subsidence structures forming the central San Juan caldera cluster, exhibits remarkable preservation of its constructional morphology, attributed to erosional exhumation by the Rio Grande over the past few million years (Steven et al., 1995; Rye et al., 2000). Its symmetrical resurgent profile, characterized by structural dips and a well-defined apical graben, aligns with other resurgent calderas in the western United States (Steven and Ratté, 1965). Moreover, its topographic caldera rim, significantly larger than its structural margin, bears witness to large-scale gravitational landsliding during eruption, subsequently modified by erosion (Larsen and Crossey, 1996). This paper will shed a light on evidence that the temperature was once colder than it is today since the ikaite precipitation was well preserved at the water column of the caldera lake.

2.3. Creede Caldera as a Saline Lake

Following the cessation of Snowshoe Mountain eruptions, Creede caldera transformed into a steep-walled, flat-floored closed basin, rapidly accumulating volcaniclastic sediments, primary volcanic deposits, and water (Larsen and Crossey, 1996; Heiken et al., 2001; Larsen and Nelson, 2000). Early caldera-filling processes involved mass wasting from unstable caldera walls, documented by conglomerates and sedimentary breccia deposits interbedded with fine-grained alluvial and shallow-lake sediments of the Creede Formation (Larsen and Nelson, 2000). Various depositional environments, predominantly lacustrine, but including alluvial near the base, facilitated the deposition of sediments, primarily below the wave base (Larsen and Nelson, 2000). The lake depth fluctuated, suggesting dynamic environmental conditions during its existence (Larsen and Crossey, 1996).

The Creede Formation predominantly comprises intermediate to felsic fallout ash, tuffaceous siltstone and limestone, and sandstone and conglomerate deposits, representing a spectrum of shallow-to-deep-water lake deposits (Larsen and Crossey, 1996). Marginally, breccia, conglomerate, and sandstone deposits attest to ancient colluvial, alluvial, and deltaic environments surrounding the shallowing caldera lake (Larsen, 1994b; Larsen and Crossey, 1996). Larsen and Lipman (2016) extensively explored the unique location of the Creede formation, focusing on the high-quality epithermal Ag-Pb-Zn deposits found there. Their research delved into the volcanic context and the Creed formation, uncovering contentious evidence of ikaite in the Lake Creede environment. They proposed the existence of pseudomorphs after ikaite in both lake sediments and tufa formations, hence, introducing the paleolimnology of ancient Lake Creede (Figure 4). This research provides valuable insights into

the geological processes and history of the region, particularly regarding the formation of mineral deposits and the environmental conditions of ancient Lake Creede.

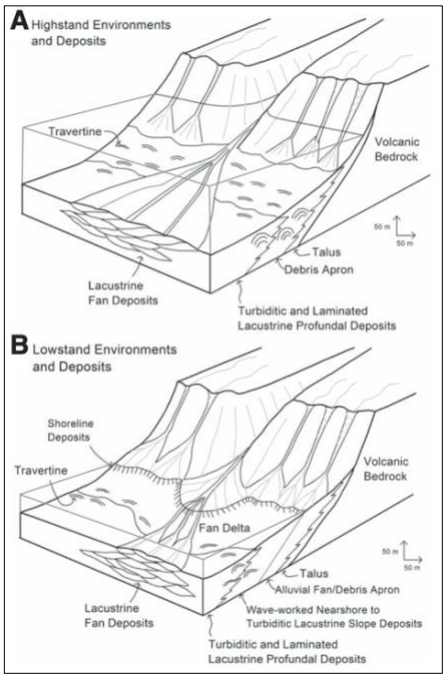

Figure 4. Proposed sketch of Creed caldera lake as the depositional environment. Area of interest where ikaite was initially form is close to the water column interface. (A) highstand and (B) lowstand lake conditions. (Modified after Larsen and Crossey, 1996).

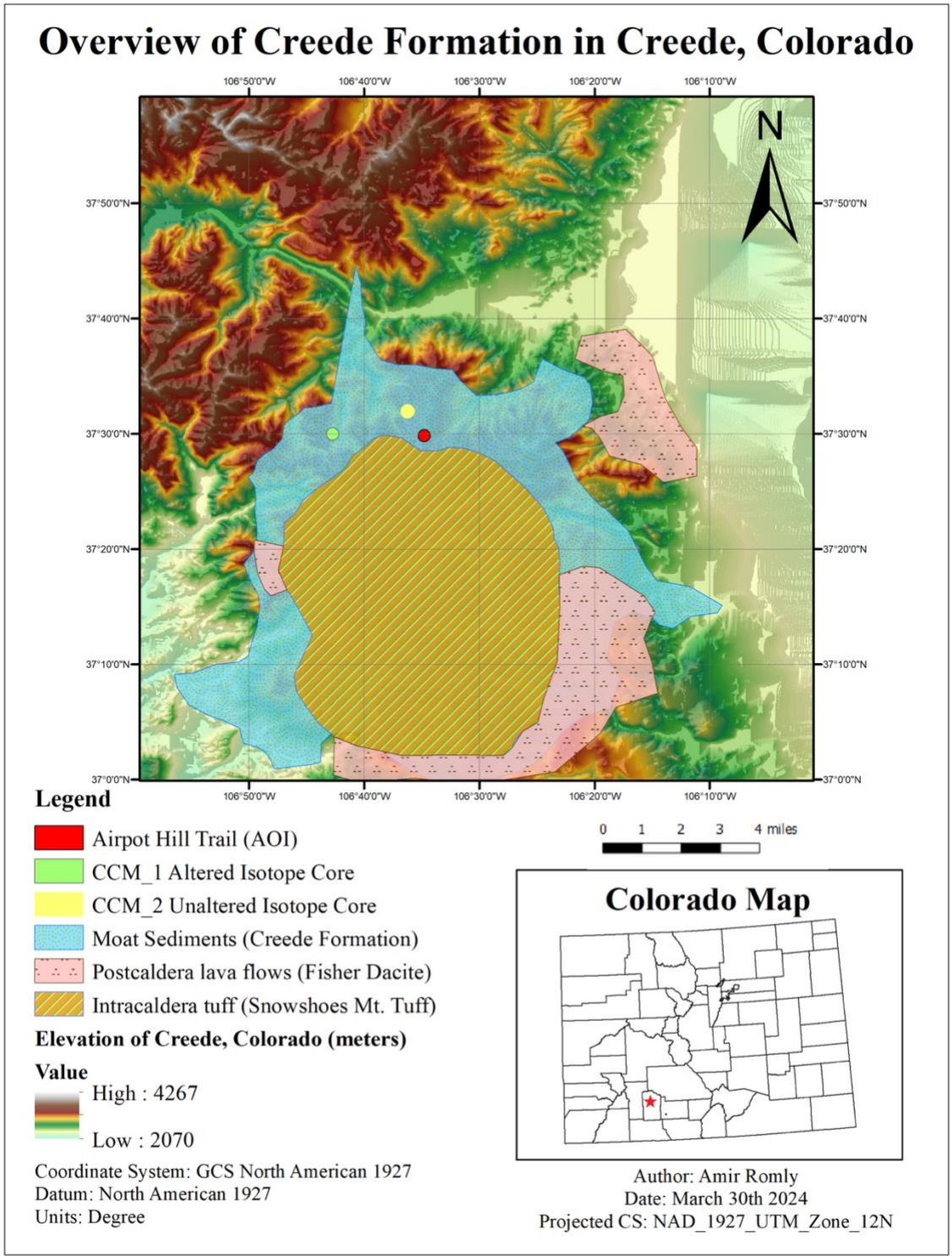

Figure 5. A simplified illustration of study area within the Creede Caldera. The map is modified after Larsen and Lipman (2016) and their study which indicated by CCM-1 and CCM-2 cores. Our four samples were obtained from Airport Hill Trail similar to their field location. (37°49.75′N, 106°55.10′W)

2.4. Climate Condition in the North America During Oligocene.

The Eocene (56 Ma to 33.9 Ma) and Oligocene (33.9 Ma to 23.03 Ma), along with their transition about 30 Ma, represent one of the most significant climate changes during the Cenozoic Era, marking a shift from a "greenhouse" to an "ice house" climate. However, studies on Oligocene climate remain ambiguous due to the shift include the opening of marine gateways, reductions in atmospheric CO_2 concentrations and/or changes in continental latitude.

Zanazzi et al. (2007) studied the climate in North America by analyzing skeletal fossils, such as teeth from mammals found in northwestern Nebraska, southwestern South Dakota, and eastern Wyoming. The fossils examined included species such as *Mesohippus* (an ancestral horse), *Merycoidodon* (a sheep-sized artiodactyl), *Leptomeryx* (a small artiodactyl), and *Subhyracodon* (an ancestral rhino). Despite not having specimens from Creede, Colorado, the fossils found in the proximate regions provide suitable proxies to understand past climate conditions.

Zanazzi et al. (2007) analyzed the $\delta^{18}O$ and $\delta^{13}C$ values of these skeletal fossils; these analyses yielded several significant findings. They found that the mean annual range of temperature (MART) changed significantly across the Eocene-Oligocene transition (EOT), with a mean annual temperature (MAT) drop of approximately 8°C. The minimum estimates of MAT were as follows: MAT (Eocene) = 21.0 ± 10.1°C, MAT (Oligocene) = 13.1 ± 9.5°C, and MAT (EOT) = 8.2 ± 3.1°C. This drop suggests that cold-month mean temperatures in the Oligocene approached freezing, indicating a substantial cooling trend during this period.

A recent investigation conducted by Straume et al. (2022) provides insights to the cause of the transition to colder climates during the Oligocene period. The study proposes that fluctuations in the Earth's interior, particularly pulsations in the Iceland mantle plume, played a

significant role in triggering climatic shifts around 33.9 million years ago and the onset of glaciations. These pulsations altered the bathymetry of the Greenland-Scotland Ridge, impacting deep water formation in the North Atlantic.

The Straume et al. (2022) model simulations suggest that changes in the Atlantic-Arctic oceanic gateways contributed to cooling, initially affecting the Southern Hemisphere and later extending to the Northern Hemisphere. This, in turn, facilitated the growth of major land-based ice sheets. These findings complement the prevailing understanding that declining atmospheric CO_2 levels and modifications to the Southern Ocean gateways or the Tethys Seaway were primary drivers of climate changes and glaciation during this period. The resultant decrease in sea temperature led to progressively colder continental climates, further advancing the transition to an "ice house" climate state during the Eocene-Oligocene transition.

III. Materials and Methods

This study used a variety of equipment, including transmitted light microscopy, cathodoluminescence, and stable isotope analyses to investigate ikaite in greater detail. Rock samples were collected from the Airport Hill hiking trail in Creede. Some of the rock samples are platy slabs that break off from the surface slope such as in Figure 6A and 4B, and other samples are more thickly bedded (Figure 6C). In the SamPLER (Sample Preparation Lab and Educational Resource) Facility in the CU Boulder Department of Geological Sciences, a Brick Rock Saw (MK 150598) was used to cut the samples into smaller pieces (Figure 6D). A Wet Tile Saw (KWS B72-06) was also used to further cut the rock in order to improve the sample's surface area (Figure 6E). When sawing rocks, it is crucial to have running water to avoid chipping the sample or overheating the rock or the saw blade. Maintaining a uniform and flat surface cut required applying strong pressure to both sides of the rock. Through this process, billets for thin sections were prepared in various sizes, including 7.5 cm by 5 cm (Figure 6F). Prepared billets were sent to Grindstone Laboratory to be prepared as polished petrographic thin sections (Figure 6G).

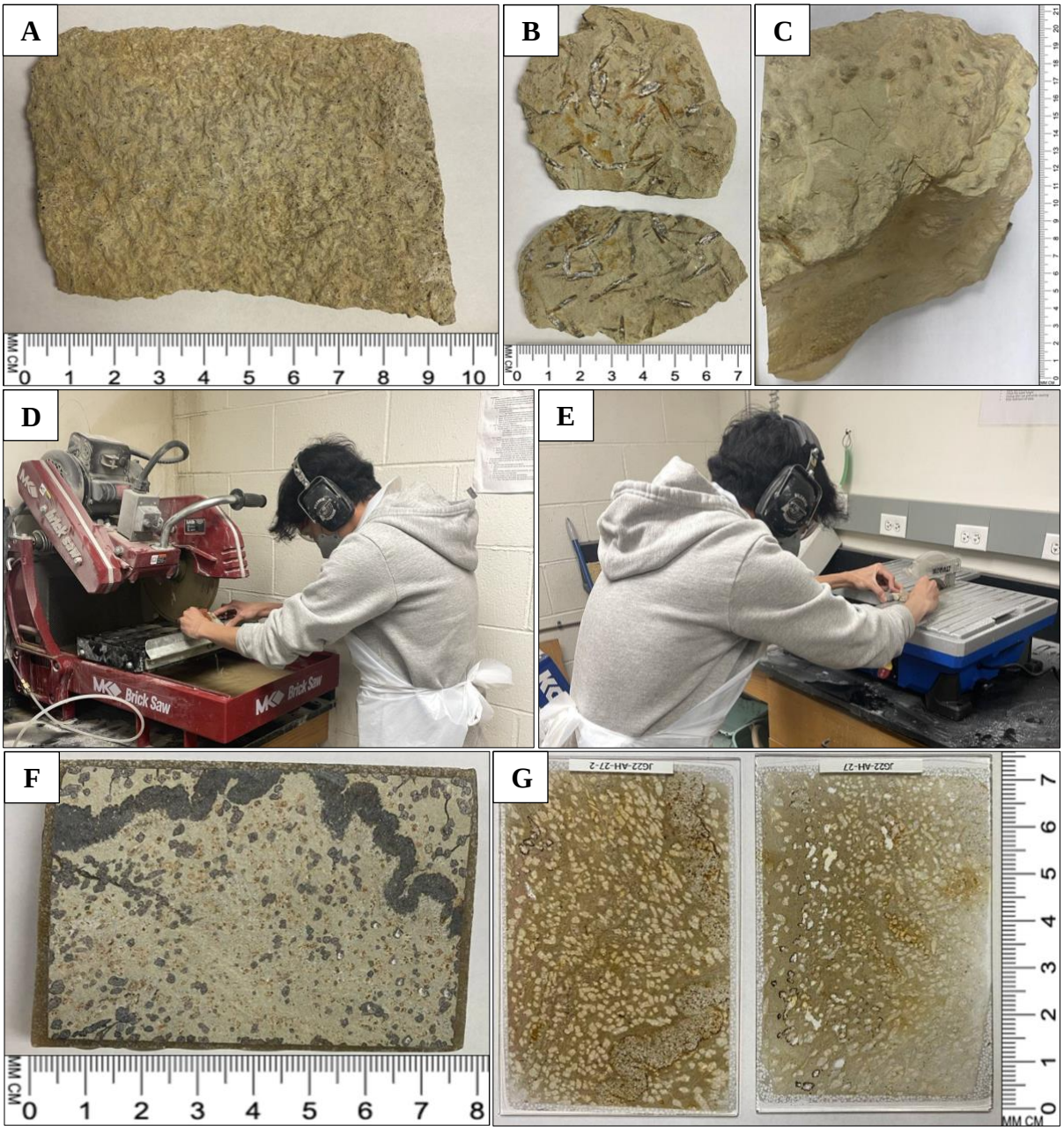

Figure 6 Images of various stages of sample processing and preparation for study. Scales are shown in centimeters (cm). **(A)** A platy rock sample exhibiting abundant carbonate crystal formations on its surface. **(B)** Dark grains of crystals containing carbonate are shown, with white striations indicating areas that were drilled for stable isotope analysis. **(C)** The sample reveals ikaite pseudomorphs embedded in a more thickly bedded rock sample. **(D)** The Brick Saw is carefully handled to cut the thickly bedded rock into smaller, manageable pieces. **(E)** The Wet Tile Saw is utilized for precision cutting of the smaller pieces into thin sections, ensuring a flat surface cut and maintaining the pristine shape of the samples. **(F)** A rock sample measuring 7.5x5cm is prepared and ready for thin section preparation. **(G)** The resulting thin section, containing microfabrics indicative of original ikaite mineralogy, ready for inspection and detailed study

1. **Transmitted Light (TL) by Zeiss Microscope**

The Zeiss Microscope (Axio Imager.M2m 3534001667) in Figure 7A enables detailed investigations of clastic, carbonate, and evaporitic rocks, aiding in the understanding of weathering and erosion processes that have shaped Earth's geological features. Here, this microscope was used for the examination of the petrography of pseudomorphs of ikaite. To begin using the microscope, the dust cover was removed. Then, the switch on the lower power supply box to the left of the microscope was turned on as shown in Figure 7B, followed by pressing the power button on the microscope itself. After startup, the stage was lowered using coarse focus and its position was adjusted with the x-y controls for slide loading.

The slide holder was handled carefully, and the slide was loaded without applying force to the stage. X-Y knobs and coarse focus were used to roughly focus the sample, adjusting the eyepiece width as necessary. Rotating the eyepieces was avoided to maintain focus. It was ensured that the light was directed to the eyepieces, not the camera. Objective controls were accessed via the touchscreen on the small panel, avoiding manual adjustments in Figure 7C. The thin sections were primarily examined under transmitted light (TL). The magnification of the objective lens varied from 5x, 10x, to 25x, depending on the scale being observed. To attain better focus, the light source was sharpened through the condenser at 25x, enhancing the depiction of crystal habits by narrowing the depth of field. Real-time examination of the thin sections using Zeiss Software (ZEN 2.3 Pro) allowed for adjustment of the microscope's brightness percentage. This ranged from 20 to 65% below the curve, thereby enhancing the visibility of guttulatic structures that may not be visible under high light intensity. Lastly the high-quality images of guttulatic crystals were captured with scale.

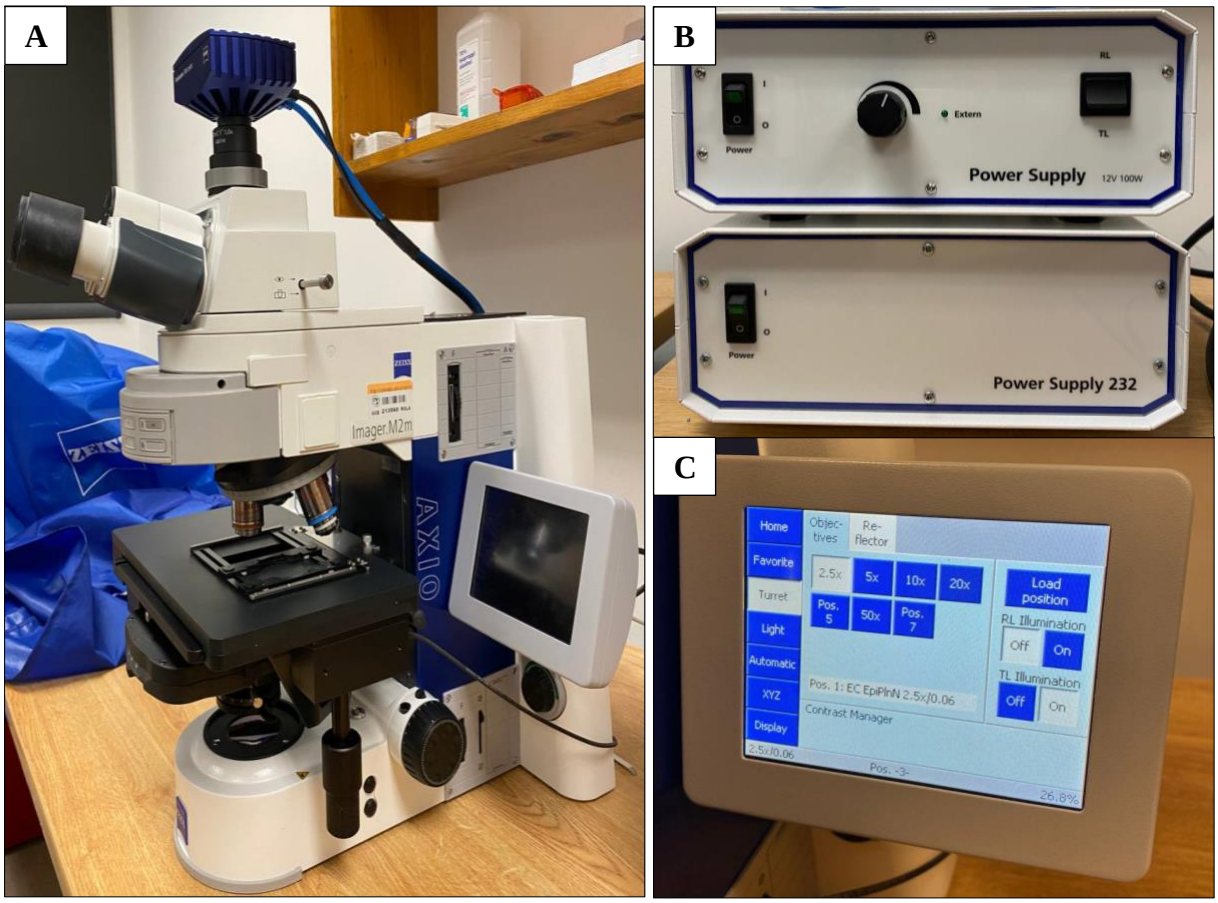

Figure 7 Images of the microscopy setup utilized for examining and imaging thin sections of rock samples. **(A)** The Zeiss Microscope (Axio Imager.M2m 3534001667) is employed for capturing Plane Polarized Light (PPL) images of the thin sections. This ensures the highest quality imaging. **(B)** While two illumination modes are available, Transmitted Light (TL) is specifically chosen for this procedure. **(C)** The system includes a small monitor, facilitating the adjustment of parameters such as changing the objective lens, loading slides, and altering light intensity via a touchscreen interface. This feature allows for precise and steady adjustments, enhancing the efficiency of the process compared to manual adjustments.

2. **Plane Polarized Light (PPL), Cross-Polarized Light (XPL) and Cathodoluminescent (CL) by CL microscope.**

Cathodoluminescence microscopy (Olympus DP73 - Model 8200 Mk II) (Figure 8A) offered three spectroscopy: Plane-Polarized Light (PPL), Cross-Polarized Light (XPL) and Cathodoluminescence (CL) that are employed in this geological research.

PPL involves passing light through a polarizing filter to create a uniform plane of vibration. When this polarized light interacts with a sample, it can reveal various optical properties such as pleochroism, which helps identify minerals and other materials based on their refractive indices. XPL enhances the contrast between different minerals by using two perpendicular polarizing filters. This technique helps highlight subtle differences in mineral composition, crystal structure, and texture, making it valuable for petrographic analysis and identifying mineral associations within rocks and thin sections. CL involves bombarding a sample with an electron beam, causing it to emit visible light. This emitted light provides information about the sample's composition, structure, and defects, making CL microscopy useful for studying ikaite crystals and other luminescent materials at the microscale.

The method began by checking that the sample chamber's leak value in the front left corner was closed. The VAC Adjust Knob on the control unit was turned slightly to the right but not tightened. Next, the control unit's Power Switch was turned on, followed by the VAC Pump Switch. To achieve a vacuum seal, the cover and door of the sample chamber had to be pressed down. An objective lens of 20x was positioned and focused on the sample (Figure 8B). The lead shield was then positioned around the objective lens. This helps to prevent ray leakage and improves concealment from surrounding lights.

When the Monitor Meter indicated a vacuum level of <0.08 Torrs, the KV ON Switch was activated. The VAC Adjust Knob was then used to regulate the beam and current. It was

critical that the gun current did not exceed 600 milliamps or drop below 150 milliamps, and that the KV ON remained between 12 and 20 KV. During operation, the VAC Adjust Knob typically needed to be adjusted to the left, periodically (Figure 8C). After that, the slide was navigated using the computer software to capture the Plane-Polarized light (PPL), Cross-Polarized Light (XPL) and Cathodoluminescent (CL) pictures. To acquire a high-quality photography and inspection, the PPL images were taken at 25-50 ms, the XPL at 50-75 ms, and the CL at 10–30 s.

After completing the procedure, the KV ON switch was turned off, followed by the VAC PUMP and POWER switches. The sample chamber's air leak valve was then opened. The microscope stage was then unlocked and lowered, making it possible to safely remove the sample. The chamber lid was reinstalled, and the microscope's transmitted light was switched off. Finally, the transformer and microscope were covered to keep them safe. This systematic shutdown procedure ensured that the equipment was properly powered off, reducing the chance of damage while conforming to safety procedures.

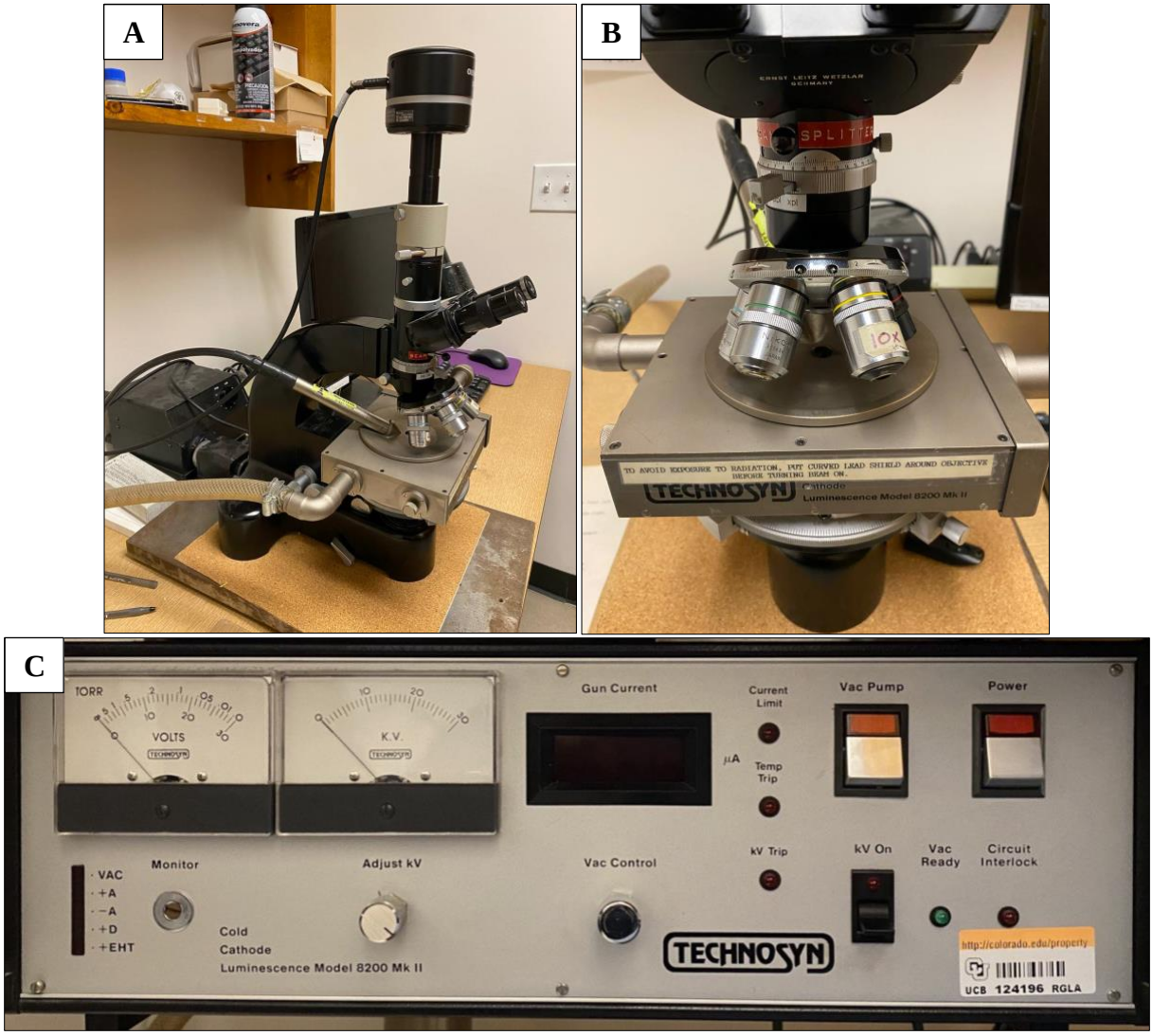

Figure 8 Images of the **(A)** Cathodoluminescent Microscope (Olympus DP73 - Model 8200 Mk II) utilized in the procedure. In **(B),** various objective lenses, typically at 20x magnification, are shown. Panel **(C)** displays the primary setup box with labeled switches used to operate the CL microscope.

3. Stable Isotope ($\delta^{13}C$ and $\delta^{18}O$) Analyses of Carbonate via Gas Bench II Analyses (GC-IRMS)

This procedure included the use of a dissecting stereomicroscope (StereoZoom SZ-4) in Figure 9A, and a microdrill (Dremel 7760) equipped with a drilling bit in Figure 9B, as well as four vials and filter paper. The selected rock sample had distinctive crystal development corresponding to rice grain form and had dark mineral components on the surface as shown in Figure 9C. The sample was then examined under 10x magnification using a stereomicroscope. Following that, the drill bit was attached to the Dremel drill, to initiate the drilling operation. Before activating the drill, it was advisable to maneuver the drill bit over the area of dark minerals under microscopic observation. This guarantees the perfect placement of the small sample. The drill was turned on once it had been properly positioned.

To expedite the procedure and assure precision, the drill was moved backward from the initial starting point, following the line of dark minerals. This operational method was crucial since it was necessary only to obtain carbonate minerals for isotopic analyses, disregarding surrounding rock matrix that was not composed of carbonate. After drilling, the sample was carefully transferred to filter paper, where a brush gently removed the remaining powdered mineral. The resulting fine material was carefully dispensed into a vial. A similar procedure was repeated for another three rock samples from the same study areas. Then, each vial was labeled as JG22-AH-27-2, JG-22-AH-23, JG22-AH-17, and JG22-AH-22 as shown in Figure 9D. The nomenclature "JG22" denoted the sample names and respective year, while "AH" designated Airport Hill Trail in Creede, with the appended 2-digit numbers indicating rocks from a specific site as designated by Larsen and Lipman (2016). The samples were weighted and proceed for the isotope processes with the partnership with Isotope Lab.

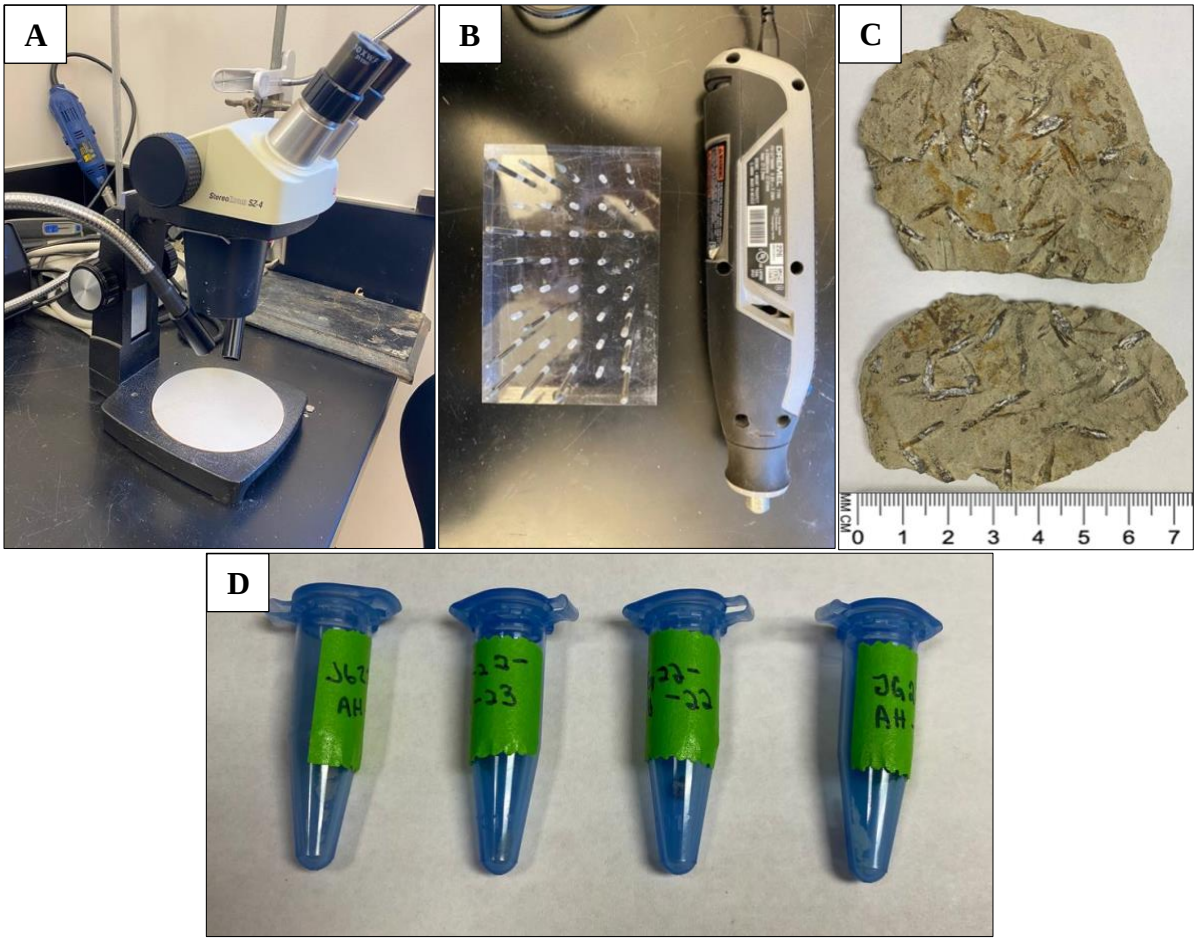

Figure 9 Images of the equipment and procedures for sample drilling and collection. **(A)** A stereomicroscope (StereoZoom SZ-4) with a 10x magnification capability is utilized to provide a clear visual for the drilling process of the samples. **(B)** The image displays a set of microdrill (Dremel 7760) and its drill bit, which is used for creating carbonate mineral powder. Smaller drill bits are for drilling of tiny crystals. **(C)** A sample exhibiting white striations shows the drilled area containing ikaite pseudomorphs. **(D)** Four vials are shown, representing powdered samples collected from four different rocks in similar sites on Airport Hill Trail.

IV. RESULTS

The results section is divided into three parts corresponding to three methods: Transmitted Light (TL) Petrography, Plane Polarized Light (PPL), Cross-Polarized Light (XPL), and Cathodoluminescence (CL) microscopy via CL Microscope, and Stable Isotope Analyses ($\delta^{13}C$ and $\delta^{18}O$) to study ikaite crystals.

1. Transmitted Light (TL) Petrography

The evidence of ikaite crystals is surprisingly unique under TL, and this finding can be observed in detail in four parts: the presence of ikaite crystals, glendonite, calcite, and deformed crystals. The primary objective in studying ikaite is to acknowledge and gain a better understanding of the crystallography that could serve as an indicator of a frigid climate. Recent research by Scheller et al. (2022) and by Žák et al. (2017) both suggest that the fabrics that form due to destabilization and replacement of ikaite crystals mainly contain hexagonal crystals with overgrowths formed as ikaite gradually dehydrates or experiences warming.

Upon investigation using Transmitted Light, it is evident that there is more variability in the formation of ikaite in the Creede Formation than described by previous researchers. Previous studies describe the typical size of guttulatic crystals as ranging from 10 to 100 μm in diameter (e.g., Scheller et al., 2022), while I observed that guttulatic crystals in the Creede sample can be from 50 to 1100μm in diameter. For example, Figures 10A and 10B depict guttulatic crystals with pseudo-hexagonal overgrowths. The hexagonal shape is less pronounced in these crystals, which slightly curve on the outside, taking on a more ellipsoidal to circular shape and 1000μm in diameter. Furthermore, I observed that the formation of ikaite can occur in various shapes during the process, such as triangular, oval, almond, teardrop, and irregular rounded cores and overgrowths (Figure 10C and 10D). This result brings new insight into recognizing the diverse

forms of ikaite, although the pseudo-hexagonal shape remains the most prominent under many circumstances.

Additionally, I observed that the guttulatic crystals occur in larger-scale ghosts with rice-grain shapes consistent with glendonite (De Lurio and Frakes, 1999; Swainson and Hammond, 2001; Selleck et al., 2007). These rice-grain-shaped crystals varied from 1600 to 2400 μm in length as seen in the glendonite stage in Figure 11 A, B, C, and D.

Given that ikaite precipitates near freezing temperatures and alters to calcite at warmer temperatures, I hypothesize that temperature disturbances in the surrounding environment may have led to the transformation of ikaite over time at the water column interface of Creede formation. Figures 12 A, B, C, and D depict examples of calcite crystals with prominent cleavage. The cleavages are particularly prominent in A and B compared to other crystals, with angles defining the faces at 78° and 102°, confirming the presence of calcite.

Lastly, an important observation is the presence of deformed ikaite crystals. Understanding the distortion of ikaite can provide insight into the event chronology or potential outcomes of ikaite exposed to its physical surroundings. For example, in Figure 13A and B, the guttulatic crystal shows signs of deformation, with the left side of the crystal broken and slightly elevated from the rest of the body, indicative of dislocation resulting from stress. The stress may be hypothesized to come from the east-west direction, allowing for thrust and breakage. Additionally, Figures 13C and D depict deformation events causing strain on the crystal from the east-west direction, followed by elongation in the north-south direction. The directions are referred to the N-S from the thin section and not the actual field location. Figure 13E reveals similar evidence, with stretching marks overlapping and intersecting the crystal cleavage.

suggesting that the deformation is in the calcite crystals which have replaced ikaite This deformation occurred after the replacement of ikaite.

1.1. Pseudo-hexagonal overgrowths as guttulatic structure in ikaite crystal

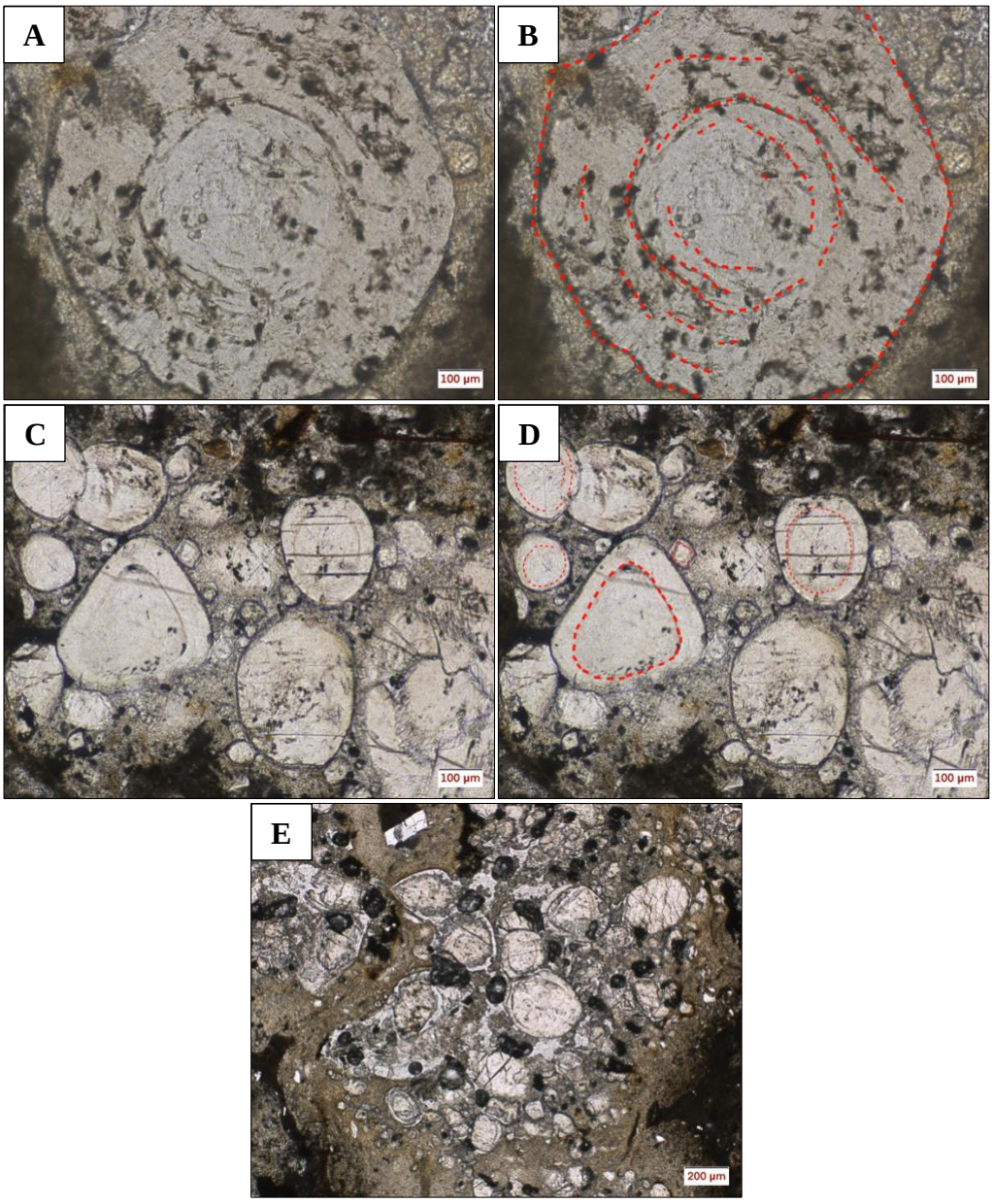

Figure 10 (A & B) show an image taken using Transmitted Light, with the 20x objective, depicting the formation of guttulatic structures with ellipsoidal overgrowths. The ellipsoidal growth is not as pronounced in these crystals, as they slightly curve on the outside, taking on a more circular shape. **(C & D)** An image taken using Transmitted Light, with the 10x objective, illustrating the variety of ikaite crystals containing triangular, oval, almond, rain drop and quadrilateral reduction overgrowths. **(F)** An image taken using Transmitted Light, using the 5x

objective, exhibiting the distinct guttulatic crystals closely interlocked with matrix of micrite, represented by the dark brown color.

1.2. The development of Glendonite as a following formation of ikaite

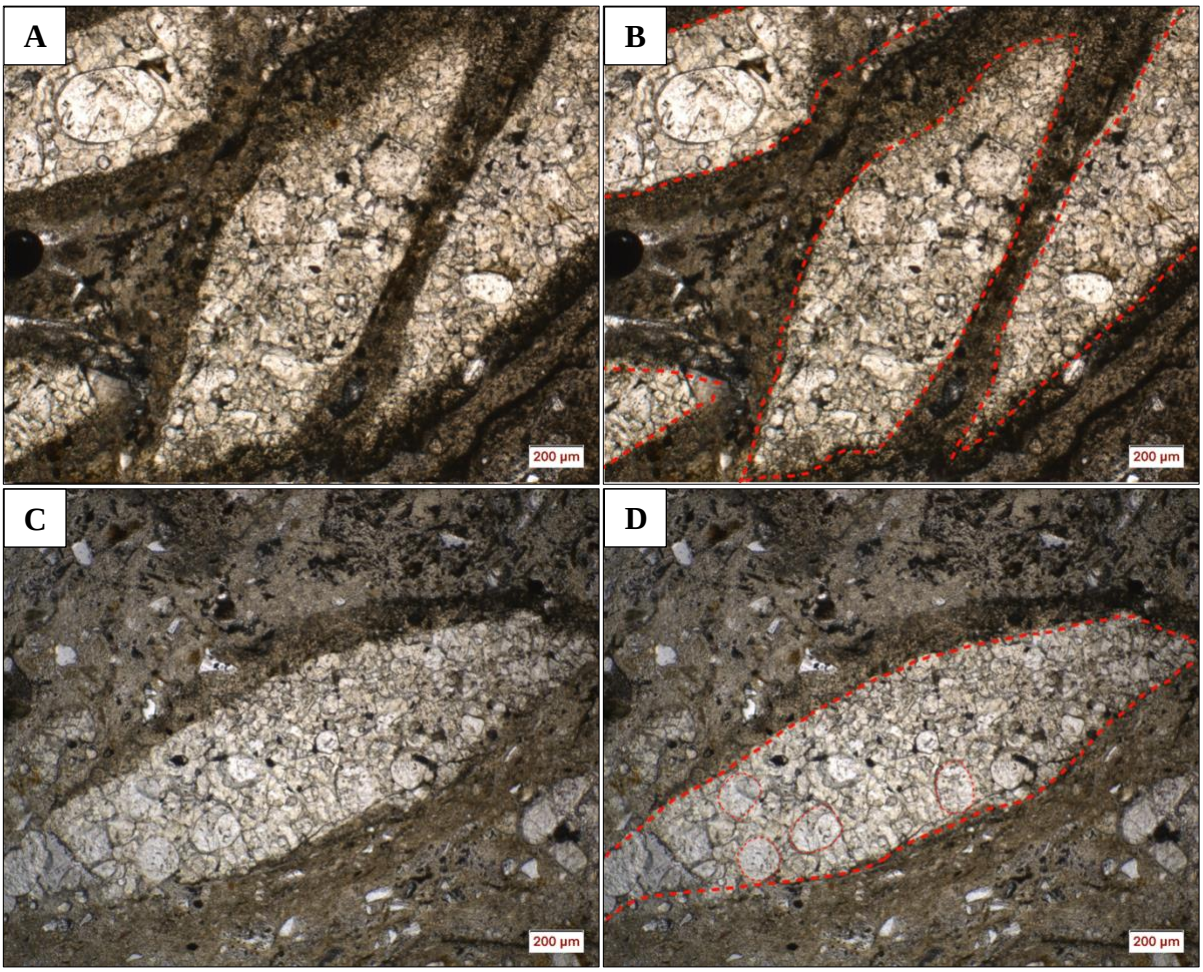

Figure 11 (**A&B**) show an image taken under Transmitted Light using the 5x objective. The individual glendonite structures, easily identified by their "rice-shaped" morphology. The brown matrix surrounding the crystals is the result of secondary micrite encircling around them. (**C&D**) An image taken under Transmitted Light, using the 5x objective. It shows a glendonite structure, with the sample taken from a farther distance in comparison to ikaite images. This is because the glendonite structures appear relatively larger compared to guttulatic crystals as it encapsuling these crystals. This size difference can be observed by noting the minuscule structure of guttulatic crystals embedded within the rice grain-like glendonite crystal.

1.3. The formation of ikaite to calcite

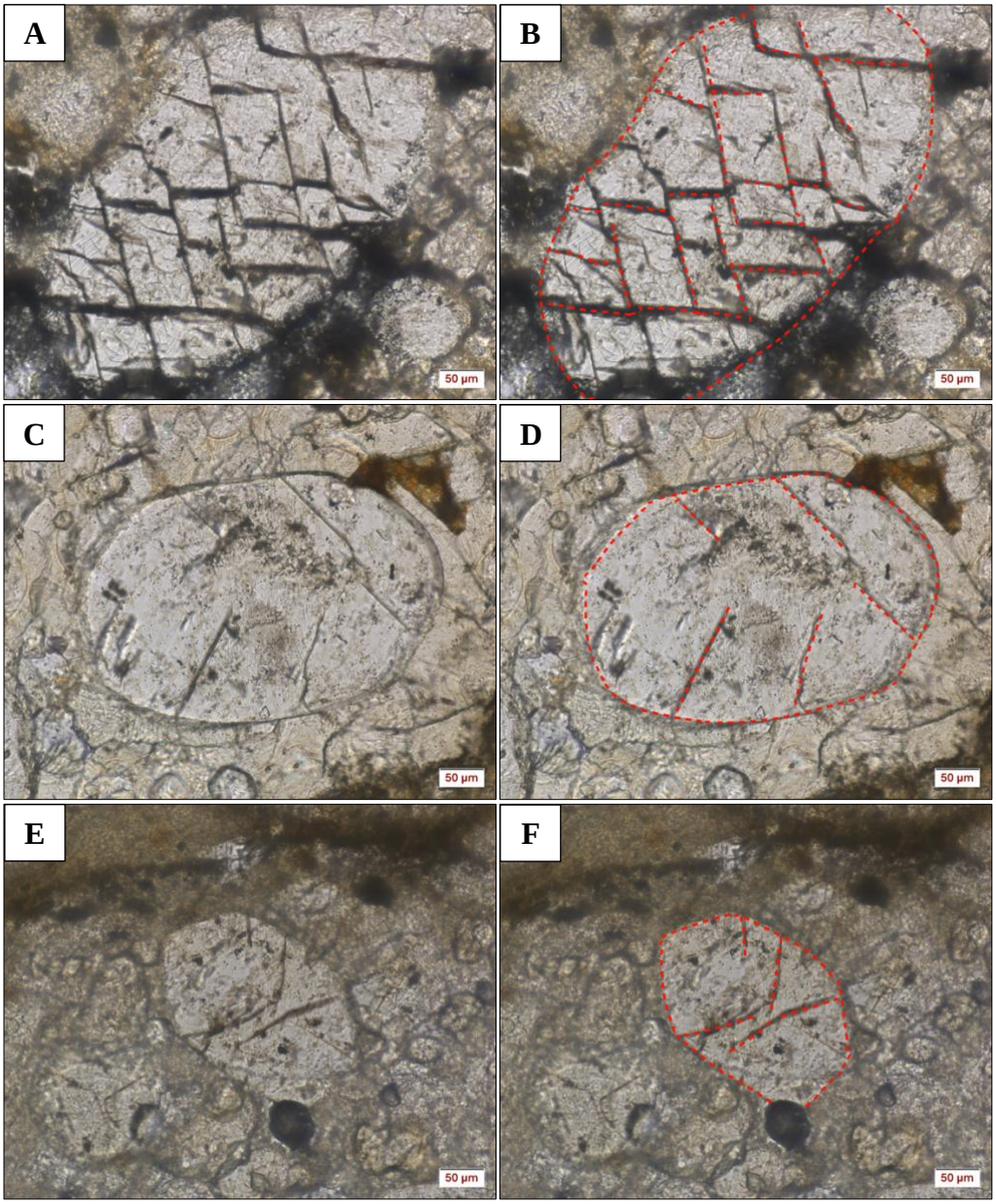

Figure 12 (A, B, C, D) were captured under Transmitted light, using the 20x objective. **Images A, B, C**, and **D** depict the formation of calcite that has replaced ikaite. The cleavages are particularly prominent in A and B compared to other crystals. These cleavages consist of diamond-shaped faces, with angles defining the faces at 78° and 102°, confirming the presence of calcite. (**E & F**) were also taken under Transmitted light, using the 20x objective. Despite the evidence of calcite formation indicated by these cleavages, the hexagonal structure of the guttulatic crystal remains intact.

1.4. The Deformation Occurrence Within Ikaite Crystal

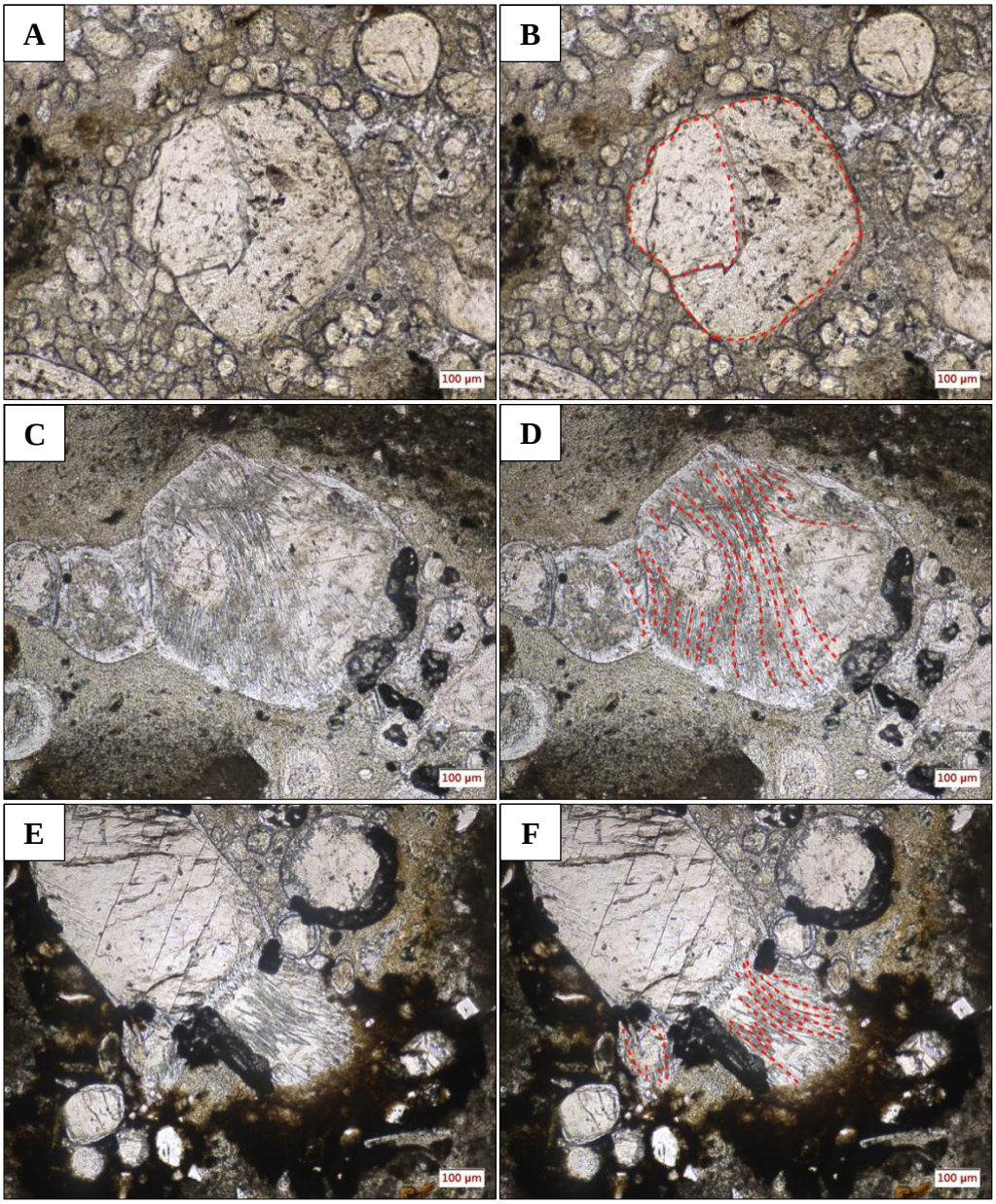

Figure 13 (A, B, C, D, E, F) were captured under Transmitted Light, using the 10x objective. **(A & B)** The ikaite crystal shows signs of deformation, where the left side of the crystal is broken and slightly elevated from the rest of the body, indicative of dislocation resulting from stress. **(C & D)** The deformation event causing strain on the crystal from the east-west direction, with subsequent elongation in the north-south direction. These directions referred to the orientation of the thin section and not the actual field location **(E & F)** Reveal similar evidence to **(C & D),** but the stretching marks overlap and intersect the cleavage of the crystal, suggesting that this deformation event may be the most recent occurrence.

2. Result: Plane Polarized Light (PPL), Cross-Polarized Light (XPL) and Cathodoluminescent (CL) by CL Microscope

The other vital aspect that can be improved to further examine the ikaite is through observing the thin-section using the Cathodoluminescent Microscope Olympus DP73 - Model 8200 Mk II. The microscope offers light modes: Plane Polarized Light (PPL), Cross-Polarized Light (XPL), and Cathodoluminescent (CL).

In Observation 1, three distinct images were captured from PPL, XPL, and CL under the 4x objective. Under PPL, there is a larger guttulatic crystal than the usual average size formed in the rock sample. The usual size is up to 200 µm; however, this crystal possesses a significant size of approximately 600 µm and has a lighter brown color. It is also surrounded by smaller guttulatic crystals (Figure 14 A, B). When observed under XPL, the crystal is not as brightly illuminated as the surrounding crystals seen in PPL. This is hypothesized to be due to the crystal's different orientation within the formation (Figure 14 C, D). Additionally, CL spectroscopy reveals overgrowths within the crystal, which are not visible under PPL and XPL. The core represents darker color followed by lighter color. The core exhibits a darker color followed by a lighter color. These changes in color indicate variations in the availability of oxygen in the sediment porewater during the formation of the guttulatic crystal (i.e., after the destabilization of ikaite). This thorough observation reveals different core shapes prevailing in circles, tear-drops, and hexagons (Figures 14 E, F).

In Observation 2, a similar procedure was conducted using the three different light modes using the 4x objective, focusing on guttulatic crystals of similar size. Under PPL, these guttulatic crystals are surrounded by a line of dark brown micrite encapsulating the crystals. This formation resembles the shape of glendonite but with less pronounced "grain-rice" shapes. Some materials similar in color to the guttulatic crystal are identified as sparry cementation, which later fills the

gaps between the guttulatic crystals. These are indicated by the green marker (Figures 15 A, B). XPL provides additional context on the cementation. Some similar guttulatic, such as the one on the upper left, do not illuminate due to the different orientation of the crystals. The sparry cementation also does not illuminate, likely due to a secondary event that occurred later or a possible different orientation preventing the cementation from being refracted under cross-polarized light (Figure 15 C, D). CL spectroscopy supports Observation 1 (Figures 14 E, F), revealing more than pseudo-hexagonal core shapes with observable ovals, tear-drops, and irregular rounded shapes (Figure 15 E, F).

The last observation focused on the clay-rich matrix around the guttulatic crystals. Images were captured using a similar procedure with the three different spectroscopy types using the 4x objective. Under PPL, the micritic matrix forming around guttulatic crystals is noted to have a dark brown color (Figure 16 A). It is hypothesized that the micrite represents adjacent sediment to the ikaite crystals. Under XPL, the cement remains opaque. This is due to the size of the micrite, which is made of tiny carbonates. Thus orienting in many ways, leading to the 'blockage of cross-polarized light. This will prevent the identification of each tiny individual micrite (Figure 16 B). Under CL, the sample shows the micritic cementation. After the guttulatic crystals form, the micrite fills in the gaps. The low amount of luminescence suggests possibility of a well oxygenated environment occurring simultaneously with the formation of the first ikaite's core (Figure 16 C).

2.1. Observation 1:

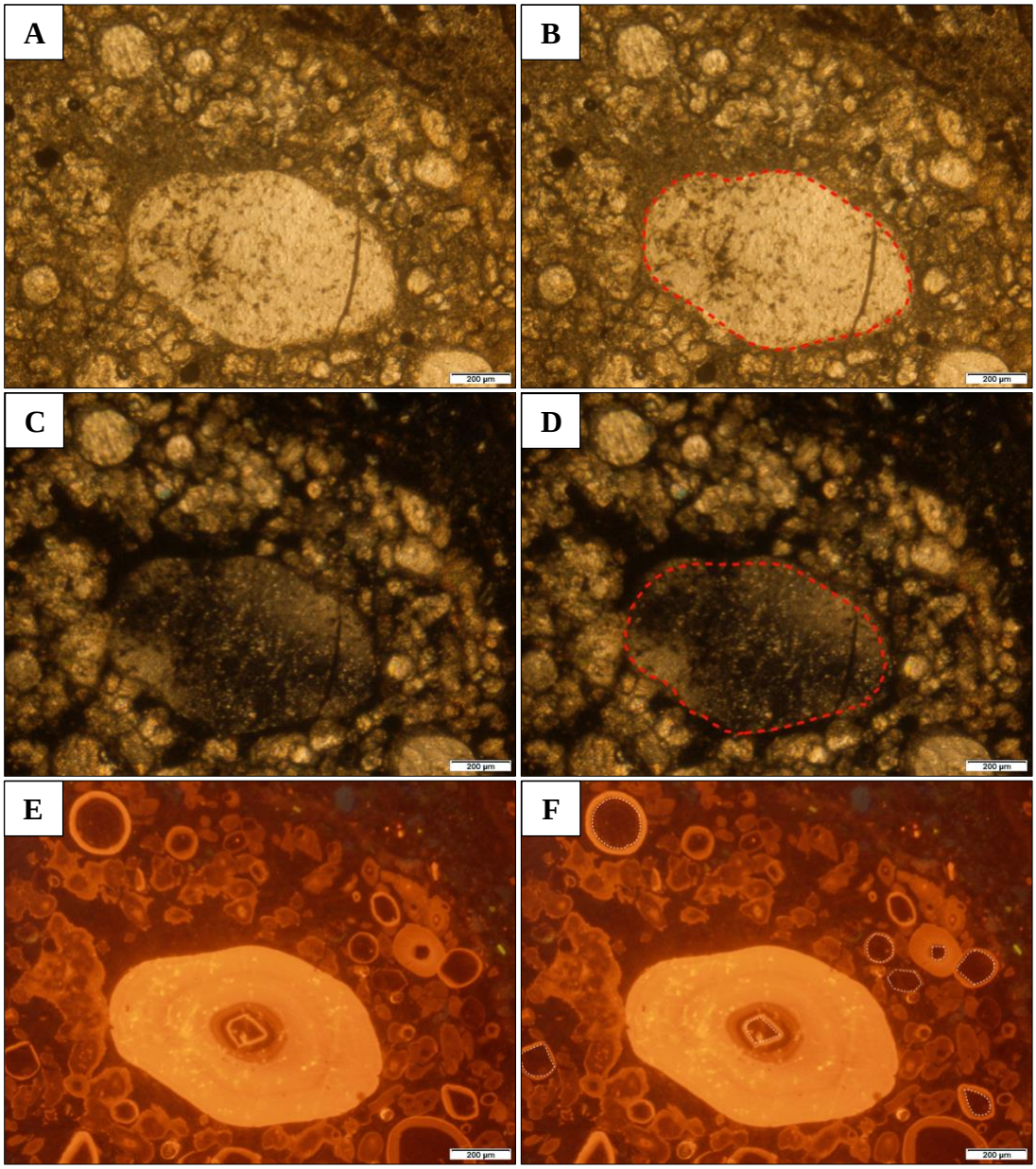

Figure 14 (A, B, C, D, E, F) were captured using the 4x objective. **(A & B)** Under PPL, the large guttulatic crystal possessed a lighter brown color surrounded by other smaller guttulatic crystals. **(C & D)** Under XPL, the prominent crystal does not illuminate due to its different orientation within the rock. **(E & F)** Under CL, some crystals that contain guttulatic fabric may not be visible but under CL, more of the ikaite crystal can observed. The dark orange color represents in the various core shapes shows that it happened first followed by lighter orange. This dark orange indicates an increase in oxygen while lighter orange indicates a depletion in oxygen during precipitation. The crystal is larger than the rest suggesting that oxygen environment prevail while guttulatic crystal formation took place.

2.2. Observation 2:

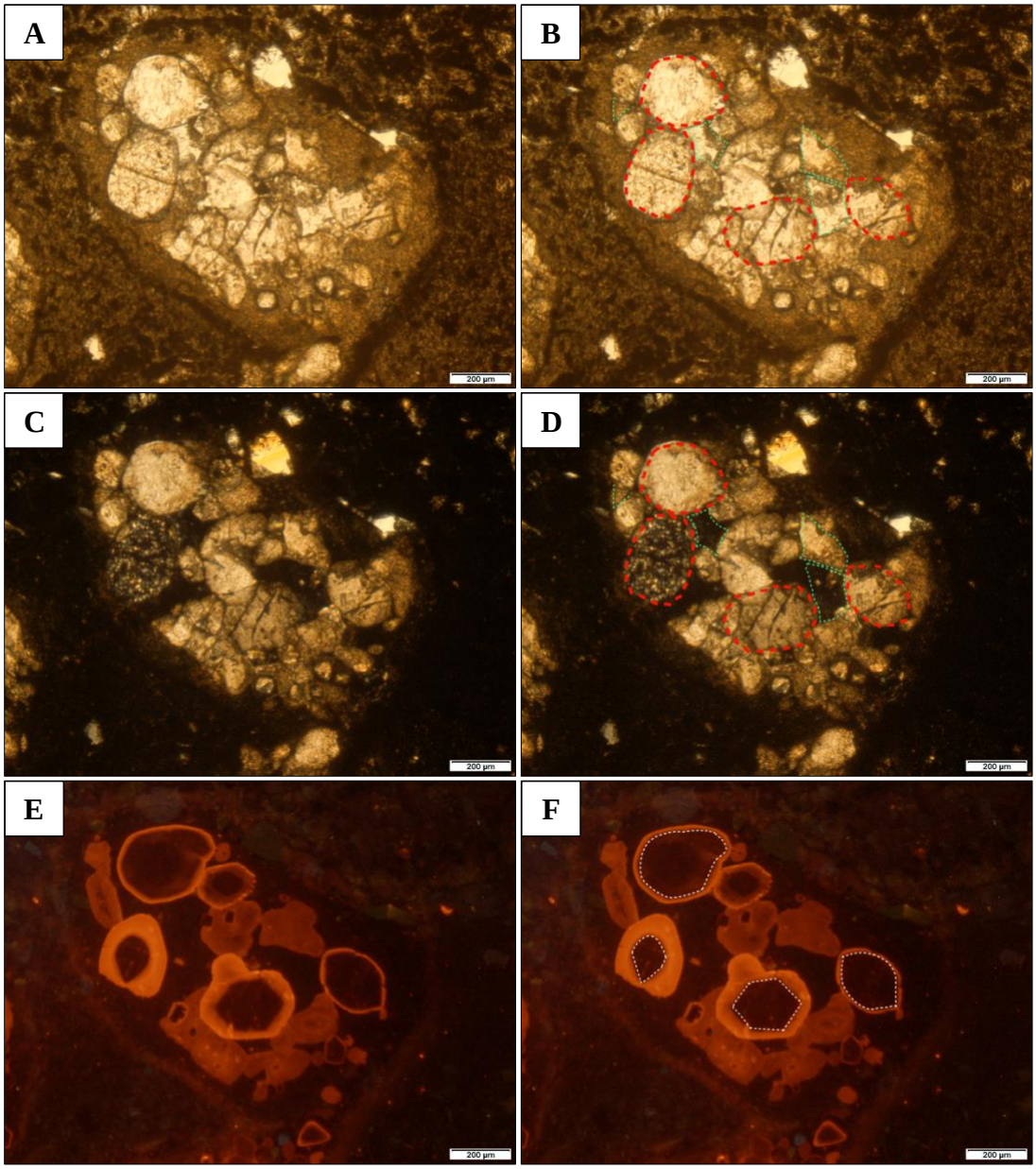

Figure 15 (A, B, C, D, E, F) show multiple ikaite crystal that were taken at using the 4x objective. **(A & B)** Under PPL, there are a few materials that has similar color to the guttulatic crystal but known as sparry cementation that later fill out the gap in between the ikaite crystal. These are shown by the green indicator. **(C & D)** Under XPL, some of the similar guttulatic crystals such as on the upper left do not illuminate due to different orientation of crystal. The sparry cementation does not illuminate due to secondary event that later took place or possible different orientation that refrain the cementation from being refracted under cross-polarized light. **(E & F)** Under CL, the summary of crystal present that was not visible in PPL and XPL are more distinct. This clearly shows the core of the crystal containing pseudo hexagonal, oval and tear drop shape. The same characteristic follows the crystal indicating darker cores formed first

during oxygen rich environment and later on with lighter orange color with oxygen depletion environment.

2.3. Cementation of Micrite Around Ikaite Crystal

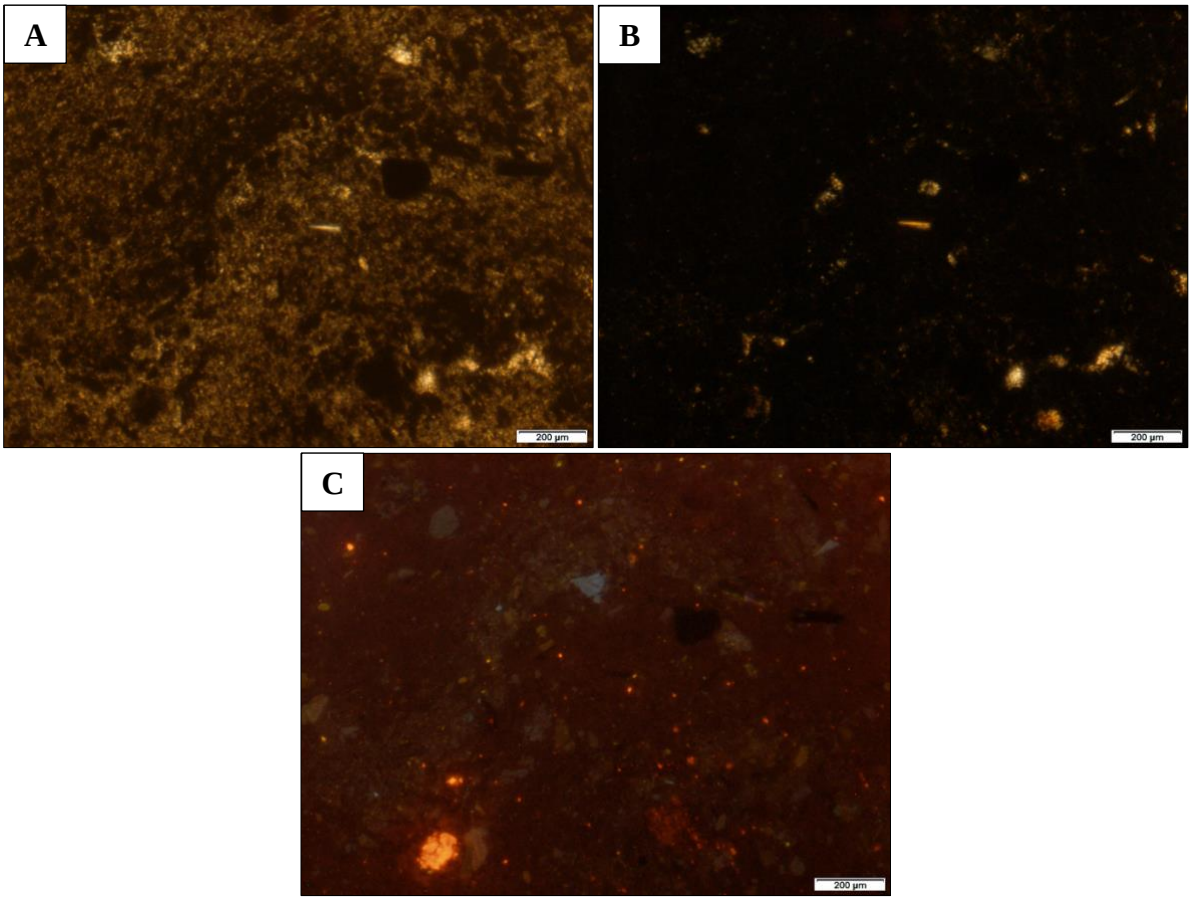

Figure 16 (A, B, C) contains the images using the 4x objective. **(A)** Under PPL, the micritic cement that form around guttulatic crystals are noted as having dark brown color. **(B)** similar image under XPL, the cement remains opaque. This is due to the size of micrite where it is made of tiny carbonates thus, they will orient in many ways which lead to blockage of cross polarized light to identify each tiny individual micrite. **(C)** Under CL, the sample shows the micrite cementation. As the ikaite crystal form, the micrite fill in between the gap which result a dull luminescence. This indicates a well oxygenated environment. There are some other colors present besides yellow/red-orange, such as dark blue and dark brown, which are indicative of other minerals.

3. Result: Stable Isotope ($\delta^{13}C$ and $\delta^{18}O$) Analyses of Carbonate via Gas Bench II Analyses (GC-IRMS)

In addition to identifying ikaite crystals using a variety of microscopy techniques, analyzing the chemical composition of $\delta^{13}C$ and $\delta^{18}O$ can provide valuable insights into past climate. Carbonate samples are commonly analyzed for stable isotopes, such as $\delta^{13}C$ and $\delta^{18}O$, using Gas Bench II Analyses and Gas Chromatography-Isotope Ratio Mass Spectrometry (GC-IRMS). This method enables the precise measurement of isotopic ratios in carbonate minerals, yielding crucial information about historical climatic conditions, paleoclimate reconstructions, and geochemical processes.

I obtained C and O isotope ratios for four samples—JG22-AH-27-2, JG-22-AH-23, JG22-AH-17, and JG22-AH-22—as shown in Figure 7D and listed in Table 1.

For $\delta^{13}C$, all four samples indicate negative values ranging from -0.58 to -3.52 ‰VPDB. In the context of carbonate analysis, negative $\delta^{13}C$ values suggest a lower abundance of the isotopically heavy carbon isotope, ^{13}C, compared to the reference material. For $\delta^{18}O$, all four samples had positive values ranging from 36.09 to 37.33 ‰VSMOW.

Table 1. $\delta^{13}C$-$\delta^{18}O$ Data for ikaite powders in glendonite

Sample	$\delta^{13}C$ ‰VPDB	$\delta^{18}O$ ‰VPDB	$\delta^{18}O$ ‰VSMOW
JG-22-AH-22	-1.02 ± 0.04	6.23 ± 0.05	37.33 ± 0.05
JG-22-AH-23	-0.60 ± 0.06	5.96 ± 0.06	37.05 ± 0.06
JG22-AH-17	-0.58 ± 0.03	6.01 ± 0.05	37.11 ± 0.05
JG22-AH-27-2	-3.52 ± 0.05	5.02 ± 0.03	36.09 ± 0.03

V. Discussion

1. Variation of Vaterite Core Chape in Guttulatic Crystal.

From the research conducted by Scheller et al. (2022), they introduced the term "guttulactic" structure, representing the pseudo-hexagonal overgrowth around the core of ikaite. Thus, the presence of ikaite crystals displaying this characteristic can infer a frigid climate of a certain location. This characteristic has been extensively observed in their research area at Mono Lake, California.

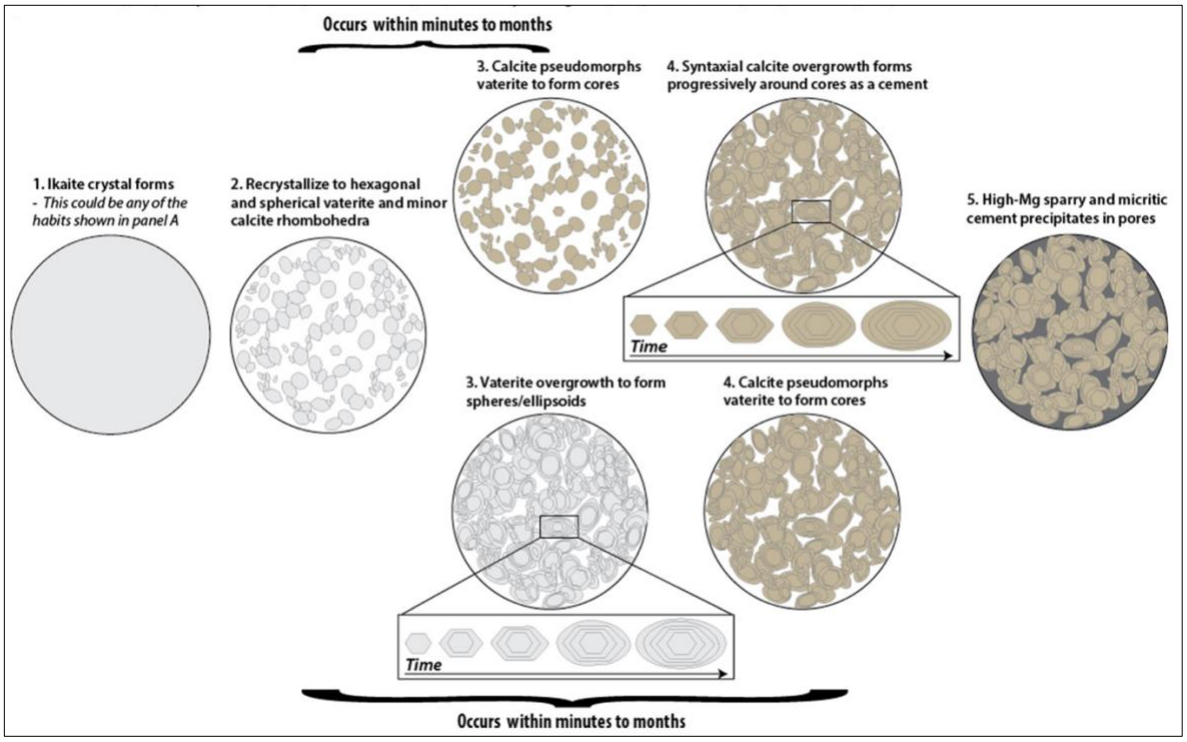

Figure 17. A chronology model for the formation of guttulatic calcite in two distinct scenarios. The syntaxial overgrowth may either be a component of the initial spherical vaterite formation, subsequently recrystallized into a single calcite crystal, or a later cement encasing calcite pseudomorphs derived from hexagonal vaterite cores. Panel A refers to Figure 2. (Modified diagram from Sheller et al. 2022)

Scheller et al. (2022) and Vickers et al. (2018) agree that since ikaite is known to be metastable, it can readily change into a stable form when minor disturbances occur. These slight changes in conditions trigger instability at the outer edge of the formation, causing ikaite to transform into vaterite, calcite, and water. Vaterite, or the guttulatic core, subsequently transitions into calcite, with calcite cement growing onto the transformed ikaite. As the process continues, subsequent layers of ikaite transform and are enveloped by growing cement. The process of changing from a hexagonal core to multiple overgrowth and eventually an ellipsoidal shape will occur within minutes to months. These pseudomorphs, which we infer as guttulatic structures, are now interlocked with one another. Ultimately, the core of ikaite undergoes transformation, followed by the continued growth of calcite, leading to the precipitation of final sparry calcite at a later stage that fills the gaps between those guttulatic structures. (Figure 17)

The study area of Creede, Colorado also exhibits evidence of pseudo-hexagonal, similar to what has been observed in Mono Lake. However, in our research, we identified a broader diversity of shapes and sizes of guttulatic structures. Scheller et al. (2022) reported vaterite with a common hexagonal core ranging from 10 to 50µm and guttulatic lengths from 10 to 100µm. In my research, by using Transmitted Light and Cathodoluminescence, I observed that the cores or vaterite formed in multiple shapes such as "tear-drop", circular, triangular, oval, and almond. The variation in core shape is ambiguous, while the hexagonal core remains dominant and abundant in the samples. Moreover, in contrast to Scheller's findings, the cores and lengths observed in my research from Creede are larger. The core sizes vary significantly, ranging from 10, 20, 50, to 100 µm. Meanwhile, the overall length of the guttulatic crystal ranges abundantly from 50 to 1100 µm. Based on my observations, the shape, core size, and length appear to be independent of each other.

2. Water Chemistry with Oxygen Content During the Guttulatic Formation.

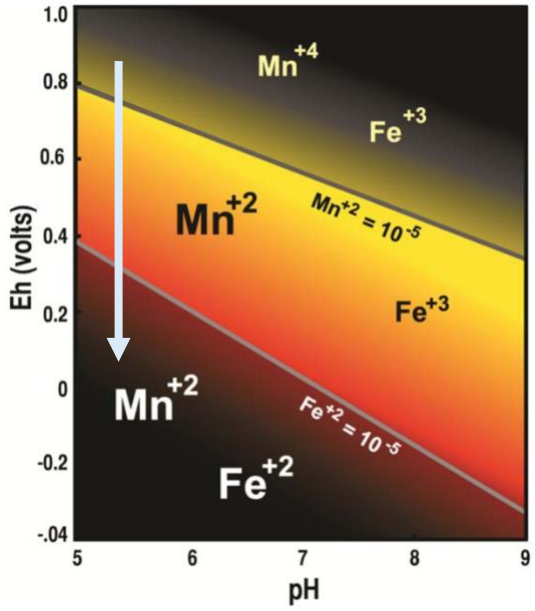

Figure 18. The distribution of Mn and Fe oxidation number in calcite under CL spectography color indicator. High Eh has higher amount of oxygen and vice versa. The arrow indicates the initial formation of vaterite to the overgrowth. (Modified after Hiatt and Pufahl, 2014)

In their study, Hiatt and Pufahl (2014) explored the application of Cathodoluminescence (CL) for calcium carbonate analysis. They noted that manganese (Mn) and iron (Fe) concentrations in carbonates serve as indicators of the redox conditions during mineral precipitation. As oxygen levels decrease, Mn is readily incorporated into diagenetic cement, followed by Fe when oxygen levels drop further. This shift is reflected in CL, with non-luminescent grains and crystal cores suggesting well-oxygenated conditions (high Eh), while brightly luminescent cement overgrowths indicate abundant Mn^{+2} but limited Fe^{+2} (low Eh). Continued decrease in oxygen levels leads to Fe^{+2} incorporation into carbonate crystals, resulting in red shades (Figure 18).

According to my Cathodoluminescence microscopy findings, the core displays a gradient from darker to lighter hues, suggesting fluctuations in oxygen availability within the sediment porewater during guttulatic crystal formation following ikaite destabilization (see Figures 14 E, F). These color variations also correlate with different Eh (Volts) and pH of water, attributed to redox reactions involved in ikaite's transformation into a stable state. The dark shade in the

vaterite core signifies a height oxygen levels (high Eh), whereas the lighter orange on the overgrowth indicates oxygen depletion during precipitation (low Eh). The high Eh to low Eh indicate the loss of oxygen process which is the reduced reaction.

When observed under Plane-Polarized Light (PPL), the micritic matrix surrounding guttulatic crystals appears dark brown (Figure 16 A), possibly representing adjacent sediment to the ikaite crystals. In contrast, under Cross-Polarized Light (XPL), the cement remains opaque due to the micrite's small carbonate composition, which leads to various orientations blocking cross-polarized light and hindering individual micrite identification (Figure 16 B). Meanwhile, under CL, the sample exhibits micritic cementation, with micrite filling in the gaps as ikaite crystals form. The minimal luminescence implies a possibly well-oxygenated environment coinciding with the initial ikaite-vaterite core formation (Figure 16 C). However, it is important to note that the dark vaterite core can be inferred as both a well-oxygenated environment (top right graph) or anoxic environment (bottom left graph).

3. Glendonite as an Ikaite Pseudomorph.

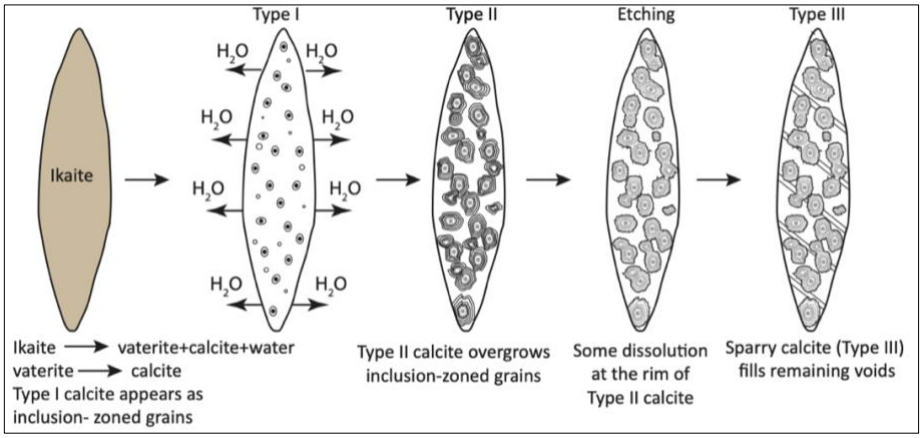

Figure 19. A chronology model of transformation from ikaite to glendonite (Modified after Vickers et al. 2018)

The term "glendonite" refers to the shape resembling rice grains. This term has been widely used in previous studies such as those by De Lurio and Frakes (1999), Swainson and Hammond (2001), and Selleck et al. (2007). Upon examination at lower magnification, the guttulatic structures are predominantly enclosed within a "rice-grained" matrix. Figure 19 illustrates the proposed transformation of guttulatic crystals as ikaite slowly changes into stable vaterite hexagonal cores with overgrowth. The overall crystal shape resembling rice grains is now identified as Glendonite.

Popov et al. (2019) described the size of glendonite to be more than 8mm and inferred it to have a prismatic chevron-like habit of stellate pseudomorph shape. However, my findings based on Transmitted Light microscopy (see Figure 11A and 9B) show smaller-sized glendonite ranging from 1.6 to 2.4 µm. Since only a few well-preserved glendonite were found in my thin sections, the actual size distribution is uncertain. Nonetheless, in conclusion, glendonite is essentially a pseudomorph of ikaite rather than an actual mineral. However, the presence of this rice grain-shaped structure offers another perspective that ikaite was initially formed, but a slight increase in temperature exceeding 8°C led to the formation of glendonite.

4. Formation of Calcite.

From the previous interpretation and literature review, it is evident that ikaite precipitates in frigid temperatures ranging from 0 to 8°C (Suess et al., 1982; Bischoff et al., 1993; Buchardt et al., 2001; Pauly, 1963; Hu et al., 2014). However, upon a rise in temperature or changes in pore-water chemistry, ikaite rapidly transforms into calcite (Pauly, 1963; Swainson and Hammond, 2001). Given that ikaite precipitates near freezing temperatures and transforms into calcite at warmer temperatures, it is hypothesized that temperature disturbances in the surrounding environment may have led to the transformation of ikaite over time at the water column interface of Creede formation.

The presence of calcite can be observed by the presence of cleavage. For calcite to form, the frigid temperature must have exceeded the stable range of ikaite, hence taking the stable state of calcite. There are two evident observations from my research that can be seen under Transmitted Light. Firstly, the 78° and 102° cleavage angle of calcite. Secondly, the calcite cleavage formed within the guttulatic crystal while still maintaining their hexagonal shape. This is consistent with my findings and demonstrates that during burial and lithification, these rocks experienced temperatures warmer than 8°C, leading to the subsequent replacement of ikaite by calcite.

5. Deformation Within Guttulatic Crystal

Another important detail within the guttulatic structure is the presence of deformation of the crystal habit. This feature is unique to the formation of ikaite in the Creede Formation. It offers valuable insights into event chronology or potential outcomes when ikaite is exposed to its physical surroundings. For instance, in Figures 13A and B, the guttulatic crystal exhibits signs of

deformation. The left side is broken and slightly elevated from the rest, indicating dislocation due to stress. This stress may originate from the east-west direction, causing thrust and breakage. Additionally, Figures 13 (C, D) illustrate deformation events causing strain on the crystal from the east-west direction, followed by elongation in the north-south direction. It is vital to note that these directions are referred to as N-S from the thin section and not the actual field location. Figure 13 (E) also reveals similar evidence, with stretching marks overlapping and intersecting the crystal cleavage. This suggests deformation in the calcite crystals that replaced ikaite, occurring after the replacement. The ikaite rock from the sample was dated during the Oligocene period, but the cause of the deformation remains ambiguous. Creede has experienced many uplift events, such as the late Neogene uplift that followed, along with the Rio Grande's incision, which exposed the soft intracaldera sediments in the Creede caldera. This event might have affected the crystal during the uplift event about 5 million years ago.

6. Oligocene Climate Temperature

According to Rye et al. (2000), $\delta^{13}C$ measurements reveal information about the carbon source and mechanisms involved in carbonate production. Variations in $\delta^{13}C$ values indicate changes in the carbon cycle, biological activity, and environmental conditions. Depleted $\delta^{13}C$ values imply organic carbon incorporation or influence from biogenic processes, while enriched values may indicate inputs from inorganic carbon sources. In contrast, $\delta^{18}O$ measurements provide insights into temperature changes, water composition, and precipitation conditions during carbonate formation. Changes in $\delta^{18}O$ values indicate changes in the isotopic composition of water sources, evaporation, and precipitation processes. Lower $\delta^{18}O$ values can indicate warmer temperatures, while higher values can indicate cooler conditions or evaporation.

Rye et al. (2000) analyzed stable isotope ratios of glendonites in two cores of the Creede Formation: CCM-1, taken from a core depth of 90.3 m to 176.5 m, appeared to have undergone extensive oxygen isotope exchange with meteoric water-dominated fluids, possibly during a local 17.6 Ma hydrothermal event. CCM-2, taken from a core depth of 80.7 m up to 245.4 m, did not appear to have undergone significant isotope exchange during recrystallization. To compensate for the depth difference for CCM-1 and CCM-2, samples were taken from approximately 90 m to 180m.

CCM-1 for $\delta^{13}C$ ‰VPDB with 6 rice-grains samples had an average of -7.78‰, while CCM-2 with 26 samples had an average of -3.17‰.

CCM-1 for $\delta^{18}O$ ‰ VSMOW with 6 rice-grains samples had an average of 21.33‰, while CCM-2 with 26 samples had an average of 34.55‰.

The $\delta^{13}C$ values from my four samples ranged from -0.58 to -3.52‰ with an average of -1.43‰. Even though the number of my samples is small, the $\delta^{13}C$ values is close to the CCM-2 samples from Rye et al. (2000). Rye et al. (2000) suggested that the low $\delta^{13}C$ values observed in the glendonite suggest that the precursor mineral was deposited in mud, where the isotopic composition of dissolved carbon in water was influenced by decaying organic matter.

Additionally, my $\delta^{18}O$ ‰ VSMOW values ranged from 36.09 to 37.33‰ with an average of 36.90‰, which falls closer to the reported margin for CCM-2 $\delta^{18}O$ values. I interpret that these higher $\delta^{18}O$ values suggest colder climate conditions. This is because the lighter isotope, ^{16}O, tends to evaporate more readily, leaving the heavier isotope, ^{18}O, behind. Higher ^{18}O indicates several factors such as the possibility of evaporative lake or ice formation in the proximity. For instance, during periods of high evaporation, lighter isotopes, such as ^{16}O, are preferentially evaporated, leaving behind water enriched in heavier isotopes like ^{18}O. This

process is known as fractionation. As a result, the remaining water, including precipitation and surface water bodies, becomes enriched in ^{18}O, leading to higher $\delta^{18}O$ values. Another hypothesis is in extremely cold conditions, precipitation may fall as snow and accumulate as ice, further enriching the remaining water bodies with ^{18}O. This process occurs because the lighter isotopes, including ^{16}O, are preferentially incorporated into ice crystals, leaving the remaining liquid water enriched in ^{18}O.

My interpretation is consistent with that of Rye et al. (2000), who suggested that $\delta^{18}O$ values in the lake were influenced by evaporation. Rye et al. (2000) observed significant and consistent $\delta^{18}O$ values observed across all carbonates (including glendonites, peloids, and microsparites).

In conclusion, the $\delta^{13}C$ and $\delta^{18}O$ values I observed are consistent with the CCM-2 data from Rye et al. (2000), indicating that my samples did not undergo significant isotope exchange during the recrystallization of ikaite to a stable state, and that the $\delta^{18}O$ values does indicate a cold-water environment.

VI. Conclusion

This research had covered for all the three methods of TL, CL with PPL and XPL, and $\delta^{13}C$ and $\delta^{18}O$ analyses to study the unique crystallography of ikaite in helping to identify the frigid ancient climate of Creede, Colorado during the Oligocene. The main importance highlight is this study provides another alternative in identifying guttulatic crystals that are petrographic fingerprints of ikaite. Previous research has argued that pseudo-hexagonal cores with overgrowths are the only characteristic microstructure that form from the destabilization of ikaite. However, my observations from the Creede Formation reveal a variety of different core shapes such as tear-drop, oval, triangular, circular almond, and irregular with rounded corners.

Apart from that, the water chemistry of ancient Lake Creede is difficult to interpret. Based on the non-luminescent core of ikaite, which is characteristic of vaterite, we hypothesize that it was formed during a high oxygenated environment. Later on, the overgrowths with lighter orange luminescence indicate a less well-oxygenated environment. Since the core is non-luminescent, it is inconclusive to determine if the environment was actually high or low oxygen during the initial formation of ikaite with the images from CL alone. However, a further test to see the high content of which Mn or Fe can confirm level of oxygen for that environment.

To strengthen the understanding about Creede, the presence of calcite with a cleavage of 78° and 102° confirmed the transformation of ikaite that only stable at temperatures cold temperature has now exceeding 8°C at the shallow water column interface of the ancient lake. Another significant evident that help to understand the behavioral of Creede Formation is the deformation within guttulatic crystals offers insights into past uplifted event during Neogene and Rio Grande incision events as stressors affecting crystal habit.

Finally, $\delta^{13}C$ and $\delta^{18}O$ values were consistent with previous studies, indicating a cold-water environment during the Oligocene. Low $\delta^{13}C$ values are consistent with the presence of organic carbon incorporation or influence from biogenic processes such as the precursor mineral was deposited in mud, where the isotopic composition of dissolved carbon in water was influenced by decaying organic matter. Higher $\delta^{18}O$ values suggest colder climate conditions, by the presence of cold and dry of evaporative ancient Creede Lake that persist about 26.9 million years ago.

VII. References

Bethke, P. M., & Hay, R. L. (2000). Overview: Ancient Lake Creede. In *Geological Society of America eBooks* (pp. 1–8). https://doi.org/10.1130/0-8137-2346-9.1

Bischoff, J. L., Stine, S., Rosenbauer, R. J., Fitzpatrick, J., & Stafford, T. W. (1993). Ikaite precipitation by mixing of shoreline springs and lake water, Mono Lake, California, USA. *Geochimica Et Cosmochimica Acta*, *57*(16), 3855–3865. https://doi.org/10.1016/0016-7037(93)90339-x

Buchardt, B., Israelson, C., Seaman, P., & Stockmann, G. (2001). Ikaite Tufa towers in Ikka Fjord, Southwest Greenland: their formation by mixing of seawater and alkaline spring water. *Journal of Sedimentary Research*, *71*(1), 176–189. https://doi.org/10.1306/042800710176

Buchardt, B., Seaman, P., Stockmann, G., Vous, M., Wilken, U., Düwel, L., Kristiansen, A., Jenner, C., Whiticar, M. J., Kristensen, R. M., Petersen, G. H., & Thorbjørn, L. (1997). Submarine columns of ikaite tufa. *Nature (London)*, *390*(6656), 129–130. https://doi.org/10.1038/36474

De Lurio, J. L., & Frakes, L. A. (1999). Glendonites as a paleoenvironmental tool: implications for early Cretaceous high latitude climates in Australia. *Geochimica Et Cosmochimica Acta*, *63*(7–8), 1039–1048. https://doi.org/10.1016/s0016-7037(99)00019-8

Dempster, T. J., & Jess, S. (2015). Ikaite pseudomorphs in Neoproterozoic Dalradian slates record Earth's coldest metamorphism. *Journal of the Geological Society*, *172*(4), 459–464. https://doi.org/10.1144/jgs2015-018

Field, L., Milodowski, A. E., Shaw, R. P., Stevens, L. A., Hall, M., Kilpatrick, A. D., Gunn, J., Kemp, S. J., & Ellis, M. A. (2017). Unusual morphologies and the occurrence of

pseudomorphs after ikaite (CaCO3·6H2O) in fast growing, hyperalkaline speleothems. *Mineralogical Magazine*, *81*(3), 565–589. https://doi.org/10.1180/minmag.2016.080.111

Geology and ore deposits of the Creede district, Colorado. (1923). https://doi.org/10.3133/b718

Heiken, G., Krier, D., & McCormick, T. C. (2001). Structural resurgence and intracaldera volcanism - Creede Caldera, Colorado. *Open-file Report (United States Geological Survey. 1978)*. https://doi.org/10.3133/ofr94260d

Hu, Y., Wolf-Gladrow, D., Dieckmann, G., Völker, C., & Nehrke, G. (2014). A laboratory study of ikaite (CaCO3·6H2O) precipitation as a function of pH, salinity, temperature and phosphate concentration. *Marine Chemistry*, *162*, 10–18. https://doi.org/10.1016/j.marchem.2014.02.003

Huggett, J., Schultz, B. P., Shearman, D. J., & Smith, A. J. (2005). The petrology of ikaite pseudomorphs and their diagenesis. *Proceedings of the Geologists' Association*, *116*(3–4), 207–220. https://doi.org/10.1016/s0016-7878(05)80042-2

Jafarzadeh, A. A., & Burnham, C. P. (1992). Gypsum crystals in soils. *Journal of Soil Science (Oxford)*, *43*(3), 409–420. https://doi.org/10.1111/j.1365-2389.1992.tb00147.x

James, N. P., Narbonne, G. M., Dalrymple, R. W., & Kyser, T. K. (2005). Glendonites in Neoproterozoic low-latitude, interglacial, sedimentary rocks, northwest Canada: Insights into the Cryogenian ocean and Precambrian cold-water carbonates. *Geology (Boulder, Colo.)*, *33*(1), 9. https://doi.org/10.1130/g20938.1

Larsen, D. (1994). Origin and Paleoenvironmental Significance of Calcite Pseudomorphs after Ikaite in the Oligocene Creede Formation, Colorado. *Journal of Sedimentary Research, Vol. 64A*. https://doi.org/10.1306/d4267e1a-2b26-11d7-8648000102c1865d

Larsen, D., & Crossey, L. J. (1996). Depositional environments and paleolimnology of an ancient caldera lake: Oligocene Creede Formation, Colorado. *Geological Society of America Bulletin*, *108*(5), 526. https://doi.org/10.1130/0016-7606(1996)108

Larsen, D., & Lipman, P. W. (2016). Exploring the ancient volcanic and lacustrine environments of the Oligocene Creede caldera and environs, San Juan Mountains, Colorado. In *Geological Society of America eBooks* (pp. 1–40). https://doi.org/10.1130/2016.0044(01

Lipman, P. W., & McIntosh, W. C. (2008). Eruptive and noneruptive calderas, northeastern San Juan Mountains, Colorado: Where did the ignimbrites come from? ˜ *the œGeological Society of America Bulletin/Geological Society of America Bulletin*, *120*(7–8), 771–795. https://doi.org/10.1130/b26330.1

Lipman, P. W., Zimmerer, M. J., & McIntosh, W. C. (2015). An ignimbrite caldera from the bottom up: Exhumed floor and fill of the resurgent Bonanza caldera, Southern Rocky Mountain volcanic field, Colorado. *Geosphere*, *11*(6), 1902–1947. https://doi.org/10.1130/ges01184.1

Lu, Z., Rickaby, R. E. M., Kennedy, H., Kennedy, P., Pancost, R. D., Shaw, S., Lennie, A., Wellner, J. S., & Anderson, J. B. (2012). An ikaite record of late Holocene climate at the Antarctic Peninsula. *Earth and Planetary Science Letters*, *325–326*, 108–115. https://doi.org/10.1016/j.epsl.2012.01.036

Morales, C., Rogov, M., Wierzbowski, H., Ershova, V., Suan, G., Adatte, T., Föllmi, K. B., Tegelaar, E., Reichart, G., De Lange, G. J., Middelburg, J. J., & Van De Schootbrugge, B. (2017). Glendonites track methane seepage in Mesozoic polar seas. *Geology (Boulder, Colo.)*, *45*(6), 503–506. https://doi.org/10.1130/g38967.1

Nelson, C. E. (2000). Volcanic domes and gold mineralization in the Pueblo Viejo district, Dominican Republic. *Mineralium Deposita*, *35*(6), 511–525. https://doi.org/10.1007/s001260050258

Pauly, H. (1963). "Ikaite", a New Mineral from Greenland. *Arctic*, *16*(4), 263. https://doi.org/10.14430/arctic3545

Peckmann, J. (2017). Unleashing the potential of glendonite: A mineral archive for biogeochemical processes and paleoenvironmental conditions. *Geology*, *45*(6), 575–576. https://doi.org/10.1130/focus062017.1

Popov, L. E., Álvaro, J. J., Holmer, L. E., Bauert, H., Pour, M. G., Dronov, A. V., Lehnert, O., Hints, O., Männik, P., Zhang, Z., & Zhang, Z. (2019). Glendonite occurrences in the Tremadocian of Baltica: first Early Palaeozoic evidence of massive ikaite precipitation at temperate latitudes. *Scientific Reports (Nature Publishing Group)*, *9*(1). https://doi.org/10.1038/s41598-019-43707-4

Rye, R. O., Bethke, P. M., & Finkelstein, D. (2000). Stable isotope evolution and paleolimnology of ancient Lake Creede. In *Geological Society of America eBooks* (pp. 233–265). https://doi.org/10.1130/0-8137-2346-9.233

Scheller, E. L., Grotzinger, J. P., & Ingalls, M. (2022). Guttulatic calcite: A carbonate microtexture that reveals frigid formation conditions. *Geology (Boulder, Colo.)*, *50*(1), 48–53. https://doi.org/10.1130/g49312.1

Schubert, C. J., Nürnberg, D., Scheele, N., Pauer, F., & Kriews, M. (1997). 13 C isotope depletion in ikaite crystals: evidence for methane release from the Siberian shelves ? *Geo-Marine Letters*, *17*(2), 169–174. https://doi.org/10.1007/s003670050023

Schultz, B. P., Huggett, J., Ullmann, C. V., Kassens, H., & Kölling, M. (2023). Links between Ikaite Morphology, Recrystallised Ikaite Petrography and Glendonite Pseudomorphs Determined from Polar and Deep-Sea Ikaite. *Minerals*, *13*(7), 841. https://doi.org/10.3390/min13070841

Selleck, B., Carr, P. F., & Jones, B. G. (2007). A Review and Synthesis of Glendonites (Pseudomorphs after Ikaite) with New Data: Assessing Applicability as Recorders of Ancient Coldwater Conditions. *Journal of Sedimentary Research*, *77*(11), 980–991. https://doi.org/10.2110/jsr.2007.087

Shearman, D. J., & Smith, A. J. (1985). Ikaite, the parent mineral of jarrowite-type pseudomorphs. *Proceedings of the Geologists' Association*, *96*(4), 305–314. https://doi.org/10.1016/s0016-7878(85)80019-5

Steven, T. A., & Ratté, J. C. (1965). Geology and structural control of ore deposition in the Creede district, San Juan Mountains, Colorado. *U.S. Geological Survey Professional Paper*. https://doi.org/10.3133/pp487

Stevens, L. E., Ayers, T. J., Bennett, J., Christensen, K. M., Kearsley, M. J. C., Meretsky, V. J., Phillips, A. B., Parnell, R. A., Spence, J. R., Sogge, M. K., Springer, A. E., & Wegner, D. L. (2001). PLANNED FLOODING AND COLORADO RIVER RIPARIAN TRADE-OFFS DOWNSTREAM FROM GLEN CANYON DAM, ARIZONA. *Ecological Applications*, *11*(3), 701–710. https://doi.org/10.1890/1051-0761(2001)011

Straume, E. O., Nummelin, A., Gaina, C., & Nisancioglu, K. H. (2022). Climate transition at the Eocene–Oligocene influenced by bathymetric changes to the Atlantic–Arctic oceanic gateways. *Proceedings of the National Academy of Sciences of the United States of America*, *119*(17). https://doi.org/10.1073/pnas.2115346119

Strohm, S. B., Saldi, G. D., Mavromatis, V., Schmahl, W. W., & Jordan, G. (2023). A study on Ikaite growth in the presence of phosphate. *Aquatic Geochemistry*, *29*(4), 219–233. https://doi.org/10.1007/s10498-023-09418-z

Suess, E., Balzer, W., Hesse, K., Müller, P., Ungerer, C. A., & Wefer, G. (1982). Calcium Carbonate Hexahydrate from Organic-Rich Sediments of the Antarctic Shelf: Precursors of Glendonites. *Science (New York, N.Y.)*, *216*(4550), 1128–1131. https://doi.org/10.1126/science.216.4550.1128

Swainson, I. P., & Hammond, R. P. (2001). Ikaite, CaCO3·6H2O: Cold comfort for glendonites as paleothermometers. ˜ *the œAmerican Mineralogist*, *86*(11–12), 1530–1533. https://doi.org/10.2138/am-2001-11-1223

Trower, E. J., Gutoski, J. R., Wala, V. T., Mackey, T. J., & Simpson, C. (2023). Tonian Low-Latitude marine ecosystems were cold before Snowball Earth. *Geophysical Research Letters*, *50*(5). https://doi.org/10.1029/2022gl101903

Vickers, M. L., Watkinson, M., Price, G. D., & Jerrett, R. (2018). An improved model for the ikaite-glendonite transformation: evidence from the Lower Cretaceous of Spitsbergen, Svalbard. *Norwegian Journal of Geology (Print Ed.)*. https://doi.org/10.17850/njg98-1-01

Wang, Z., Chen, C., Wang, J., Suess, E., Chen, X., Ma, X., Wang, G., & Xiao, S. (2020). Wide but not ubiquitous distribution of glendonite in the Doushantuo Formation, South China: Implications for Ediacaran climate. *Precambrian Research*, *338*, 105586. https://doi.org/10.1016/j.precamres.2019.105586

Zanazzi, A., Kohn, M. J., MacFadden, B. J., & Terry, D. O. (2007). Large temperature drop across the Eocene–Oligocene transition in central North America. *Nature (London)*, *445*(7128), 639–642. https://doi.org/10.1038/nature05551

Zhou, X., Lu, Z., Rickaby, R. E. M., Domack, E. W., Wellner, J. S., & Kennedy, H. (2015). Ikaite abundance controlled by porewater phosphorus level: potential links to dust and productivity. *The Journal of Geology*, *123*(3), 269–281. https://doi.org/10.1086/681918

VIII. Acknowledgement

Completing this research has been made possible by the invaluable support and guidance of several individuals and groups to whom I owe immense gratitude. I am deeply thankful to Dr. Lizzy Trower for inviting me to join the Chemical Sedimentology Research Group at CU Boulder and for her mentorship, guidance, and unwavering belief in my abilities. I am also grateful to Dr. Kathryn Snell, Dr. Ashley Maloney, and Dr. Miquela Ingalls (PSU) for their invaluable assistance with geochemical analysis and their expertise, insights, and support throughout this research. My heartfelt appreciation goes to the lab members, including Jim Gutoski, Brianna Hibner, Juliana Olsen-valdez, Cedric Hagen, Nicole Mizrahi, Tyler Lincoln, and others, for their dedication, collaboration, and assistance. I would like to thank Dr. Zawaski for input on structural deformation analysis. Additionally, I extend my gratitude to my family, friends, and siblings for their continuous support, encouragement, and understanding. Overall, I am profoundly grateful for the contributions, guidance, and support of all involved, which have had a profound impact on both my academic and personal growth. It has been a privilege to collaborate with such exceptional individuals on this research endeavor.